MOLECULAR BIOLOGY

Mature mRNA processing that deletes 3′ end sequences directs translational activation and embryonic development

Yuki Takada[1,2], Ludivine Fierro[1], Keisuke Sato[1], Takahiro Sanada[1], Anna Ishii[1], Takehiro Yamamoto[3], Tomoya Kotani[1,2]*

Eggs accumulate thousands of translationally repressed mRNAs that are translated into proteins after fertilization to direct diverse developmental processes. However, molecular mechanisms underlying the translation of stored mRNAs after fertilization remain unclear. Here, we report a previously unknown RNA processing of 3′ end sequences of mature mRNAs that activates the translation of stored mRNAs. Specifically, 9 to 72 nucleotides at the 3′ ends of zebrafish *pou5f3* and mouse *Pou5f1* mRNAs were deleted in the early stages of development. Reporter assays illustrated the effective translation of the truncated forms of mRNAs. Moreover, promotion and inhibition of the shortening of 3′ ends accelerated and attenuated Pou5f3 accumulation, respectively, resulting in defective development. Identification of proteins binding to unprocessed and/or processed mRNAs revealed that mRNA shortening acts as molecular switches. Comprehensive analysis revealed that >250 mRNAs underwent this processing. Therefore, our results provide a molecular principle that triggers the translational activation and directs development.

INTRODUCTION

Protein-coding genes in eukaryotes are transcribed by RNA polymerase II, and nascent precursor mRNAs (pre-mRNAs) are subsequently processed through coordinated nuclear events, such as 5′ capping, splicing, 3′ cleavage, and polyadenylation (*1*). In particular, splicing and 3′ cleavage are responsible for defining the accurate length and sequence of mature mRNAs by selecting exons and the 3′ cleavage site of pre-mRNAs. The resultant mature mRNAs are exported to the cytoplasm and translated by ribosomes. In recent decades, studies have shown that numerous mRNAs are not immediately translated; their translation is spatially and temporally regulated in the cytoplasm of various cells in diverse organisms (*2*–*4*). Therefore, protein synthesis is generally regulated at the level of translation and transcription. However, the biological significance and molecular mechanisms of posttranscriptional regulation in most cases remain unexplored.

Zebrafish and mouse oocytes accumulate approximately 8000 mRNAs (*5*–*7*), of which >2000 mRNAs are stored as translationally repressed mRNAs (*6*, *8*–*10*). As transcription remains quiescent immediately before fertilization until zygotic genome activation (ZGA) at the 1000-cell stage in zebrafish and 2-cell stage in mice (*7*, *11*, *12*), the temporal regulation of protein synthesis after fertilization is achieved via translational activation of dormant mRNAs stored in eggs. Although the time of translation of distinct mRNAs and the underlying mechanism remain largely unknown, both inhibition and promotion of global translation have been demonstrated to cause defects in diverse developmental processes, including ZGA, embryonic axis formation, and cell differentiation (*13*–*17*). Therefore, the temporal regulation of global translation is crucial for the appropriate promotion of early development.

Although the translational repression of mRNAs in eggs and their activation after fertilization have been reported in sea urchin embryos since the 1960s (*18*–*20*), the mechanisms underlying the temporal regulation of mRNA translation have been extensively studied during oocyte maturation in *Xenopus* using some mRNAs exhibiting dormancy in immature oocytes. Pioneering studies have demonstrated that dormant mRNAs carry short polyadenylate [poly (A)] tails in the oocyte cytoplasm and that their short length maintains a translationally inactive state in immature oocytes, which are arrested at prophase of meiosis I (*21*–*24*). After the resumption of meiosis, these dormant mRNAs undergo polyadenylation, resulting in the translational activation of mRNAs and promotion of oocyte maturation until the oocytes are arrested again at metaphase of meiosis II (*25*, *26*). Furthermore, studies using *Xenopus*, zebrafish, and mouse oocytes have revealed that the timing of the translational activation of distinct mRNAs is precisely regulated by RNA binding proteins that bind to the cis-acting elements in the 3′ untranslated region (3′UTR) (*6*, *27*–*32*).

Unlike the regulation of oocyte maturation, little is known about the mechanisms underlying the translational regulation of mRNAs after fertilization. Studies using zebrafish embryos have indicated that polysome-incorporated mRNAs are globally altered after fertilization and that most mRNAs incorporated in polysomes undergo polyadenylation (*5*, *17*). The polyadenylation of mRNAs stored in eggs is therefore suggested to be a fundamental mechanism promoting the translation of numerous mRNAs. However, the processes by which thousands of mRNAs are translated after fertilization and the molecular mechanisms temporally regulating the translation of dormant mRNAs during development remain largely unclear.

Zebrafish *pou5f3* and mouse *Pou5f1* mRNAs encode the homologous transcription factors Pou5f3 (also known as Pou2/Pou5f1) and Pou5f1/Oct4 (*33*–*35*), respectively. Zebrafish and mouse

[1]Biosystems Science Course, Graduate School of Life Science, Hokkaido University, Sapporo 060-0810, Japan. [2]Department of Biological Sciences, Faculty of Science, Hokkaido University, Sapporo 060-0810, Japan. [3]Department of Biochemistry, Keio University School of Medicine, Tokyo 160-8582, Japan.
*Corresponding author. Email: tkotani@sci.hokudai.ac.jp

oocytes were demonstrated to accumulate *pou5f3* and *Pou5f1* mRNAs, respectively, as translationally repressed mRNAs, and the translation of both mRNAs was activated after fertilization, although *Pou5f1* mRNA was partially translated in mouse mature oocytes (*36*, *37*). The generation of maternal and zygotic *pou5f3* mutants in zebrafish revealed that Pou5f3 is essential after fertilization for the differentiation of endoderm cells and specification of dorsal-ventral regions (*38*–*40*). In addition, Pou5f3 has been demonstrated to induce ZGA (*41*, *42*). Using *pou5f3* mRNA as a paradigm to study the temporal translation of dormant mRNAs after fertilization, we previously revealed the existence of a mechanism physically regulating mRNA translation, i.e., mRNA translation is persistently inhibited in oocytes by the formation of solid-like granules, and it is activated when the granules transform into liquid droplets during the cleavage stage (*37*).

In this research, we extended the study on *pou5f3* mRNA and found a previously unknown RNA processing method that activates the translation of dormant mRNAs. We revealed that the 3′ end sequences [9 to 72 nucleotides (nt)] of *pou5f3* and *Pou5f1* mRNAs were deleted before translational activation of the mRNAs in both zebrafish and mouse embryos. This 3′ end deletion directed the translational activation of mRNAs and appropriate progression of early development. The identification of proteins binding to the unprocessed or processed mRNAs revealed the function of 3′ ends as molecular switches. In addition, >40% of the 568 examined mRNAs were found to be similarly processed. Together, our results provide a molecular principle of the translational regulation of dormant mRNAs after fertilization, which directs animal development.

RESULTS

The 3′ end sequences of mature mRNAs are processed

We previously revealed that the poly(A) tails of zebrafish *pou5f3* mRNA were elongated after fertilization, but not during oocyte maturation, based on the polymerase chain reaction (PCR)–based poly (A) test (PAT) assay (*37*). To explore the molecular mechanisms by which dormant mRNA translation is activated after fertilization, we analyzed changes in the 3′ end of *pou5f3* mRNA in further detail by sequencing the PAT assay products (fig. S1A). Intriguingly, a large proportion of *pou5f3* mRNAs in oocytes had longer 3′ end sequences in the UTR than those previously isolated from gastrula-stage embryos (Fig. 1, A and B, sequences in blue) (*33*). Moreover, the 3′ end sequences of most *pou5f3* mRNAs were shortened, particularly from 2-hour post fertilization (hpf; cleavage stage) to 4 hpf (blastula stage; Fig. 1B), coinciding with the increase in protein synthesis (*37*, *43*). The number of deleted nucleotides was 68 or 72 in all stages, and the resultant 68-nt-deleted mRNA was identical to the previously isolated mRNA (*33*). The poly(A) tails of *pou5f3* mRNA were short in oocytes and slightly elongated in embryos at 0 hpf (Fig. 1B and fig. S1B). The poly(A) tails were widely elongated in mRNAs with shortened 3′ ends, but not in mRNAs with full-length 3′ ends, in embryos from 2 to 4 hpf (Fig. 1B and fig. S1B).

A previous study showed that *pou5f3* mRNA expression increased remarkably at 2 hpf (*44*), although ZGA is known to initiate at 3 hpf (1000-cell stage) (*7*, *12*). Because our previous study demonstrated that *pou5f3* mRNA form solid-like granules in fertilized eggs and transform into liquid-like droplets shortly after fertilization (*37*), we predicted that the increase in mRNA levels at 2 hpf was attributable to changes in the efficiency of RNA extraction from embryos. To address this possibility, we extracted RNAs after the degradation of protein-RNA complexes by proteinase K treatment, which increased the level of *pou5f3* mRNAs extracted from fertilized eggs (fig. S1C). The total amount of *pou5f3* mRNA was equivalent over the period from 0 to 2 hpf and slightly increased at 4 hpf (fig. S1D), suggesting the presence of zygotic *pou5f3* transcripts at 4 hpf and being consistent with the beginning of ZGA after 3 hpf. To rule out the possibility that *pou5f3* mRNA with a short 3′UTR is derived from zygotic transcription, we used single-nucleotide polymorphisms (SNPs) to distinguish zygotic mRNAs from maternal mRNAs. The homozygous genomic differences between females and males allowed us to distinguish between maternal and paternal mRNAs (fig. S2A). The PAT assay of embryos at 4 hpf revealed that almost all (95.2%) *pou5f3* mRNAs carried female SNPs (fig. S2B), suggesting the presence of a few zygotic transcripts at this stage. Next, to experimentally eliminate zygotic transcripts at 4 hpf, we inhibited transcription by treating embryos with amanitin. Amanitin treatment almost completely inhibited the transcription of zygotically expressed genes in the earliest stage (fig. S2C). The PAT assay revealed that the 3′ end of *pou5f3* mRNA was shortened even in amanitin-treated embryos (fig. S2D). Under this condition, Pou5f3 protein was accumulated at the level equivalent to that in control embryos at 4 hpf (fig. S2E). These results indicate that changes in the length of 3′ end sequences occur due to the deletion of the 3′ end sequences of maternal mRNAs; in addition, we revealed that the maternal mRNAs synthesize most Pou5f3 in early-stage embryos.

Wnt8a has been isolated as one of the candidates of dorsal axis determinant that might be synthesized from stored *wnt8a* mRNA after fertilization (*45*). In oocytes and fertilized eggs (0 hpf), approximately 50% of *wnt8a* mRNAs have long 3′ ends, and the remaining mRNAs have 93-nt-deleted 3′ ends (fig. S3, A and B). The proportion of *wnt8a* mRNAs carrying shortened 3′ ends was higher in embryos at 2 and 4 hpf, and the number of deleted nucleotides reached 99 (fig. S2, A and B). The poly(A) tails of *wnt8a* mRNA remained short in oocytes and embryos at 0 and 2 hpf but became elongated in embryos at 4 hpf (fig. S3, B and C).

We then analyzed changes in the 3′ end of *Pou5f1* mRNA (Fig. 1C) in mouse oocytes and embryos. The PAT assay indicated that the 3′ end of *Pou5f1* mRNA was shortened during oocyte maturation, which was shortly elongated in early two-cell stage embryos (Fig. 1D). Sequence analysis of the PAT assay products revealed that the 3′ end sequences of *Pou5f1* mRNA were deleted in mature oocytes and that the proportion of mRNAs with shortened 3′ ends was higher in early two-cell stage embryos (Fig. 1, C and E). Because the total amount of *Pou5f1* mRNA remains the same during this period (*36*) and zygotic transcription starts from the late two-cell stage in mice (*11*), these changes indicated the deletion of the 3′ ends of maternal mRNAs. The number of deleted nucleotides ranged from 9 to 14, and the proportion of *Pou5f1* mRNAs with shortened 3′ ends was higher in early two-cell stage embryos. The poly(A) tails of *Pou5f1* mRNA were transiently shortened in mature oocytes, which were then elongated again in two-cell stage embryos (Fig. 1, E and F).

The processed mRNA is effectively translated

Because the shortening of 3′ end sequences preceded or coincided with the synthesis of proteins encoded by the mRNAs, it was postulated that this RNA processing promotes the translational

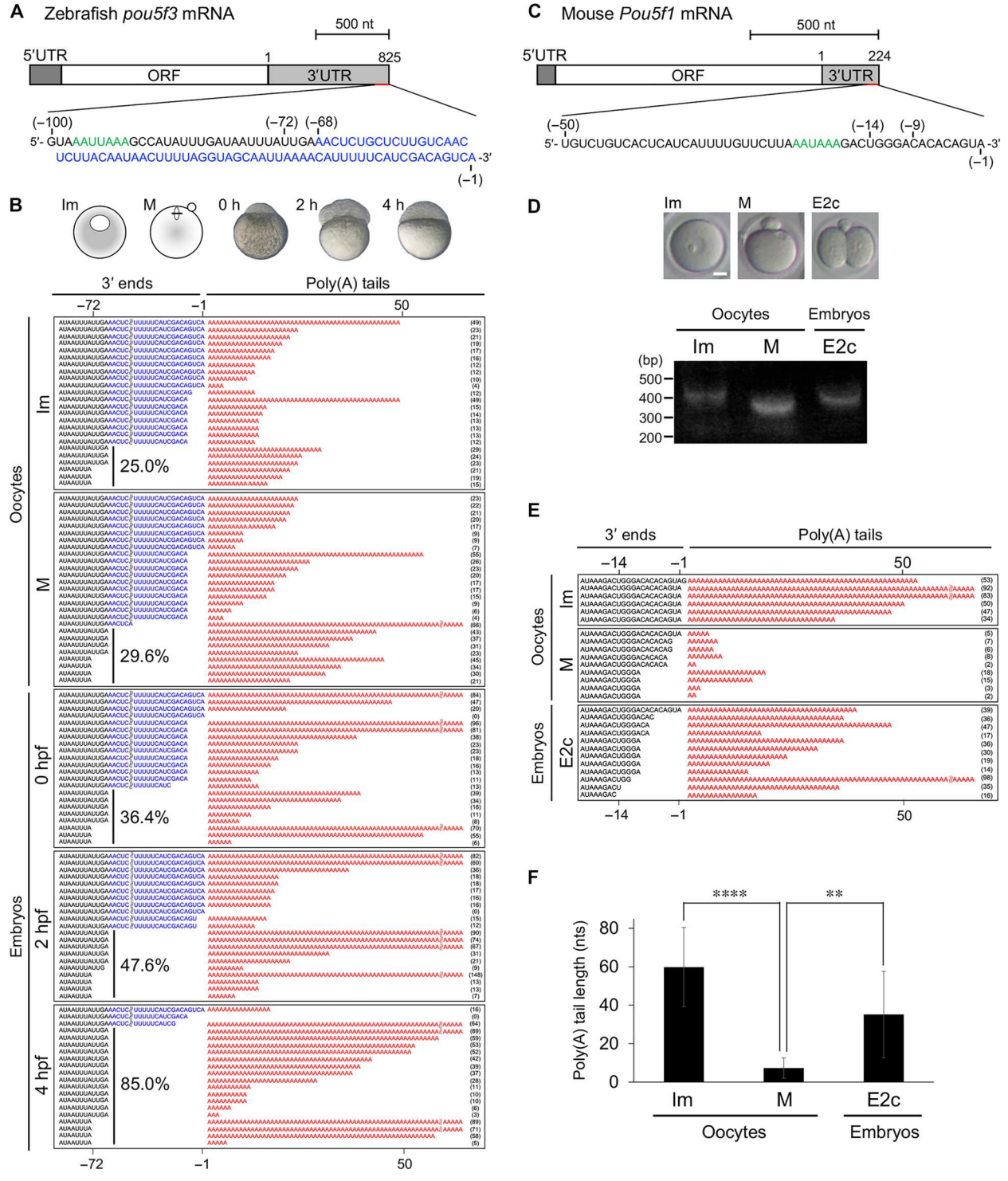

Fig. 1. The 3′ end sequences of mature mRNAs are shortened during early development in zebrafish and mice. (**A**) A schematic diagram of full-length zebrafish *pou5f3* mRNA. The 3′ end sequences (100 nt) are presented at the bottom. Sequences in blue indicate an additional 3′ end. Sequences in green denote the poly(A) signal (PAS). ORF, open reading frame. (**B**) Sequence analysis of the 3′ ends of *pou5f3* mRNA in immature (Im) and mature (M) oocytes and embryos at 0, 2, and 4 hpf. The lengths of 3′ ends (left) and poly(A) tails (right) are presented. Similar results were obtained from two independent experiments. (**C**) A schematic diagram of full-length mouse *Pou5f1* mRNA. The 3′ end sequences (50 nt) are presented at the bottom. Sequences in green denote PAS. (**D**) PAT assay for mouse *Pou5f1* mRNA in Im and M oocytes and early two-cell stage embryos (E2c). bp, base pair. Similar results were obtained from two independent experiments. Scale bar, 20 μm. (**E**) Sequence analysis of the 3′ ends of *Pou5f1* mRNA in the PAT assay. The lengths of 3′ ends (left) and poly(A) tails (right) are presented. (**F**) Lengths of *Pou5f1* poly(A) tails in the sequence analysis were determined (means ± SD). ****$P < 0.0001$ and **$P < 0.01$, Tukey's multiple comparison test.

activation of dormant mRNAs stored in eggs. To evaluate this possibility, we first established transgenic zebrafish carrying full-length (long) or shortened (short) 3′UTRs of *pou5f3* mRNA located downstream of the heat shock promoter and coding region of green fluorescent protein (GFP) (Fig. 2A). As a control, we established transgenic zebrafish carrying the simian virus 40 (SV40) 3′UTR located downstream of the GFP-coding region (Fig. 2A).

Transgenic adult females were subjected to heat shock, and their embryos were analyzed by in situ hybridization, quantitative reverse transcription PCR (RT-PCR), and puromycylation followed by the proximity ligation assay (Puro-PLA). Puro-PLA enables the detection of nascent peptides synthesized in ribosomes using two antibodies that are specific for the protein of interest and puromycin (*37*, *46*). Compared to the detection of GFP, which requires a sufficient period to exhibit fluorescence after translation (*47*), this method can directly visualize the translational activity of reporter mRNAs. In this study, heat shock induced the transcription of all reporter mRNAs at a similar level (Fig. 2B). Puro-PLA revealed that the reporter mRNA with the SV40 3′UTR was effectively translated in the cytoplasm of embryos at 2 hpf (Fig. 2, C and D). The reporter mRNA with a long *pou5f3* 3′UTR was not translated at this stage (Fig. 2, C and D), suggesting the translational repression of this reporter mRNA. Conversely, the reporter mRNA with a short *pou5f3* 3′UTR was effectively translated (Fig. 2, C and D). After 2 hours, the reporter mRNA with the long 3′UTR was partly translated (fig. S4, A and B), with shortening of some of its 3′ end sequences (fig. S4C), thereby recapitulating the regulation of endogenous *pou5f3* mRNA, although not completely. Consistent with the early activation of the reporter mRNA with the short 3′UTR, GFP was detected in these embryos by immunoblotting (fig. S4D). These results suggest that the shortening of 3′ end sequences promotes the translational efficiency of mRNA in the early stage of development.

To elucidate the relationship between 3′ end shortening and translational regulation in further detail, we analyzed the translational efficiency by injecting mouse oocytes with reporter mRNAs containing the long or short 3′UTRs of *Pou5f1*, which were located downstream of the firefly luciferase coding region (Fig. 3, A and B). We constructed reporter mRNAs carrying 9- and 14-nt deletions at the end of *Pou5f1* 3′UTRs as short 3′UTRs because the 9-nt deletion was the most frequently observed change in oocytes and embryos, and the 14-nt deletion indicated the maximum length of deletion in early cleavage-stage embryos (Fig. 1E). In immature oocytes, the reporter mRNAs carrying a short *Pou5f1* 3′UTR exhibited little or no difference in luciferase activity compared with those reporter mRNA carrying a long *Pou5f1* 3′UTR (Fig. 3C). In contrast, the luciferase activity of reporter mRNAs carrying a short *Pou5f1* 3′UTR significantly increased in mature oocytes, and this increase was dependent on the length of the deletion (Fig. 3C). The PAT assay showed that the reporter mRNA with a short, but not a long, 3′UTR was frequently polyadenylated (fig. S4E). These results suggest that the 3′ end shortening promotes the translational activation of *Pou5f1* mRNA in mature mouse oocytes.

To determine whether the sequences at the end of the 3′UTR are involved in translational regulation, we injected oocytes with reporter mRNAs carrying *Pou5f1* 3′UTRs with mutations at their 3′ end (Fig. 3, D and E). We generated 2- or 5-nt mutations in the conserved sequence of mouse and zebrafish and mutations of 9 nt that were shortened in mouse embryos (Fig. 3D). In immature oocytes,

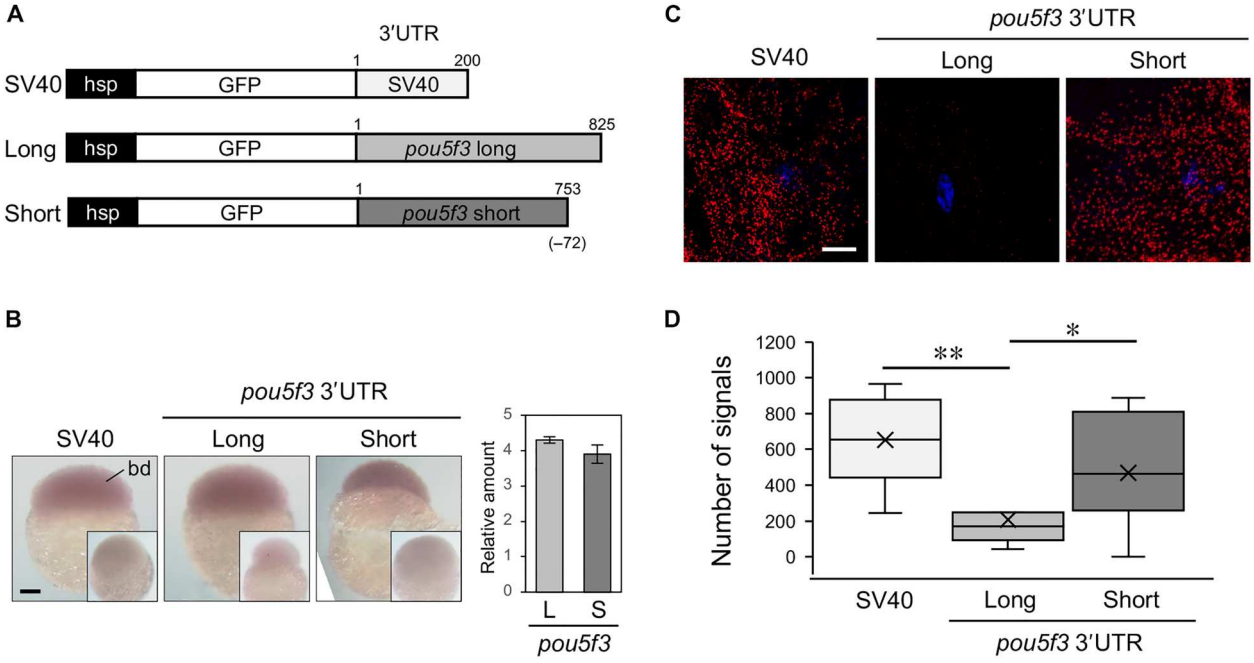

Fig. 2. Reporter mRNA with a shortened *pou5f3* 3′UTR is effectively translated in the early development of zebrafish. (**A**) Schematic diagrams of reporter genes with the SV40 3′UTR (SV40), full-length *pou5f3* 3′UTR (Long), and processed *pou5f3* 3′UTR (Short). (**B**) Left: Whole-mount in situ hybridization of reporter mRNAs in transgenic zebrafish embryos at 2 hpf with the *GFP* antisense probe. Insets are embryos hybridized with the *GFP* sense probe. bd, blastodisc. Similar results were obtained from two lines of transgenic zebrafish. Right: Reporter mRNA levels were determined by quantitative RT-PCR (means ± SD; $n = 3$). (**C**) Detection of newly synthesized GFP using Puro-PLA in embryos at 2 hpf. DNA is indicated in blue. Scale bars, 100 μm (B) and 10 μm (C). (**D**) Number of Puro-GFP PLA sites per 40,000 μm^2 was counted (means ± SD; $n \geq 18$). Similar results were obtained from three independent experiments. $^{**}P < 0.01$ and $^{*}P < 0.05$, Mann-Whitney's *U* test.

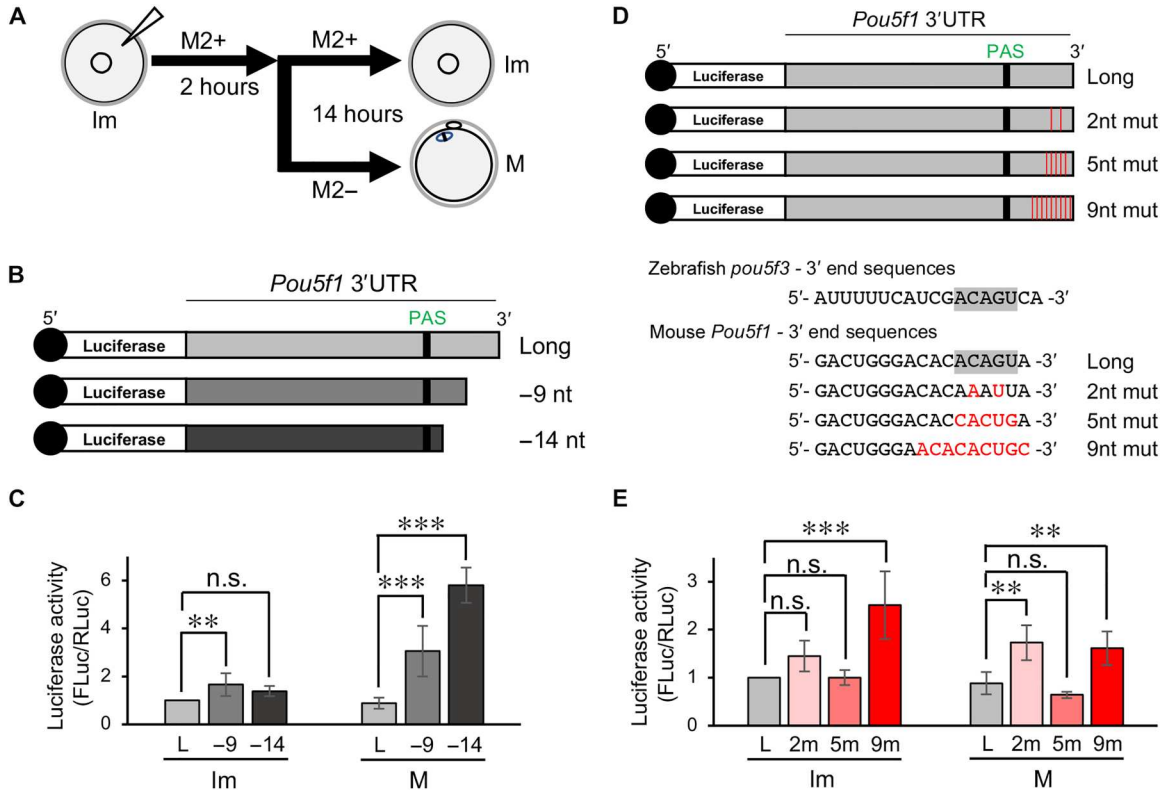

Fig. 3. The reporter mRNA with shortened *Pou5f1* 3′UTR is effectively translated in mouse mature oocytes. (**A**) A schematic diagram of the reporter assay in mouse oocytes. Immature oocytes were injected with reporter mRNAs and cultured in M2+ medium for 2 h, followed by incubation with M2+ or M2− for 14 hours. Immature (Im) and mature (M) oocytes were collected and extracted for the luciferase assay. (**B**) Schematic diagrams of reporter mRNAs with the full-length *Pou5f1* 3′UTR (Long) and 9- and 14-nt-deleted 3′UTRs (−9 and −14 nt). (**C**) Results of the luciferase assay (means ± SD; $n \geq 4$). The activities relative to that of Long mRNA in immature oocytes. ***$P < 0.001$ and **$P < 0.01$, Dunnett's test. (**D**) Schematic diagrams (top) and sequences (bottom) of reporter mRNAs carrying the full-length *Pou5f1* 3′UTR (Long) and 3′UTRs with 2-, 5-, or 9-nt mutations (2nt, 5nt, and 9nt mut, respectively). Sequences that are conserved in zebrafish and mouse are highlighted in gray. (**E**) Results of luciferase assay (means ± SD; $n \geq 3$). The activities relative to that of Long mRNA in immature oocytes. ***$P < 0.001$, **$P < 0.01$, Dunnett's test. n.s., not significant.

the luciferase activity of the reporter mRNA carrying 9-nt mutations in the *Pou5f1* 3′UTR was 2.5-fold higher than that of the reporter mRNA carrying a long *Pou5f1* 3′UTR (Fig. 3E). In mature oocytes, the luciferase activity of reporter mRNAs carrying 2- and 9-nt mutations was higher than that of the reporter mRNA carrying a long *Pou5f1* 3′UTR. However, the differences were <2-fold (Fig. 3E). These results indicate that the 3′ end sequences mainly contribute to the translational repression of *Pou5f1* mRNA in immature oocytes.

Genome editing of the *pou5f3* 3′UTR increases protein synthesis and affects embryonic development

To determine whether modifications of 3′ end sequences affect mRNA translational regulation and embryonic development, we generated mutations at the 3′ end of *pou5f3* using CRISPR-Cas9 technology. Two lines of genome-edited zebrafish were established in which 24 and 7 nt were inserted at the 3′ end, respectively (Fig. 4A). We crossed females and males that were heterozygous for the insertions and isolated fish that were homozygous for the insertions. All offspring were viable and fertile. Embryos derived from the homozygous females and males exhibited no remarkable phenotype until 4 hpf, but they displayed delays in epiboly progression during the gastrulation stage (Fig. 4B). In particular, $pou5f3^{7i/7i}$ embryos exhibited more substantial growth delay than $pou5f3^{24i/24i}$ embryos. The progression of development was severely retarded during and after gastrulation, and the larvae showed curled tails (fig. S5A) and died within 7-day post fertilization (dpf). Immunoblotting indicated that $pou5f3^{24i/24i}$ and $pou5f3^{7i/7i}$ embryos accumulated higher levels of Pou5f3 than wild-type embryos at 0 and 3 hpf (Fig. 4C and fig. S5, B to D). Consistent with the more severe phenotypes, the increase in the amounts of Pou5f3 in $pou5f3^{7i/7i}$ embryos was higher than that in $pou5f3^{24i/24i}$ mutants. Notably, according to previous studies, Pou5f3 has been detected as two different bands (*37*, *43*). In this study, we found that the band with a higher molecular weight showed remarkably increased expression in the mutants (fig. S5, B to D). These results demonstrated that insertions in the 3′ end sequences of *pou5f3* increased Pou5f3 synthesis, resulting in developmental retardation.

To explore the effect of insertions on Pou5f3 expression, the 3′ end of *pou5f3* mRNA in eggs derived from the homozygous fish was analyzed using the PAT assay. Intriguingly, the poly(A) tails of *pou5f3* mRNA appeared to be elongated in both $pou5f3^{24i/24i}$ and $pou5f3^{7i/7i}$ eggs, which was not observed in wild-type eggs (Fig. 4D and fig. S5E). Sequence analyses demonstrated the shortening of the 3′ ends of almost all *pou5f3* mRNAs in both $pou5f3^{24i/24i}$ and $pou5f3^{7i/7i}$ eggs (Fig. 4E and fig. S5F).

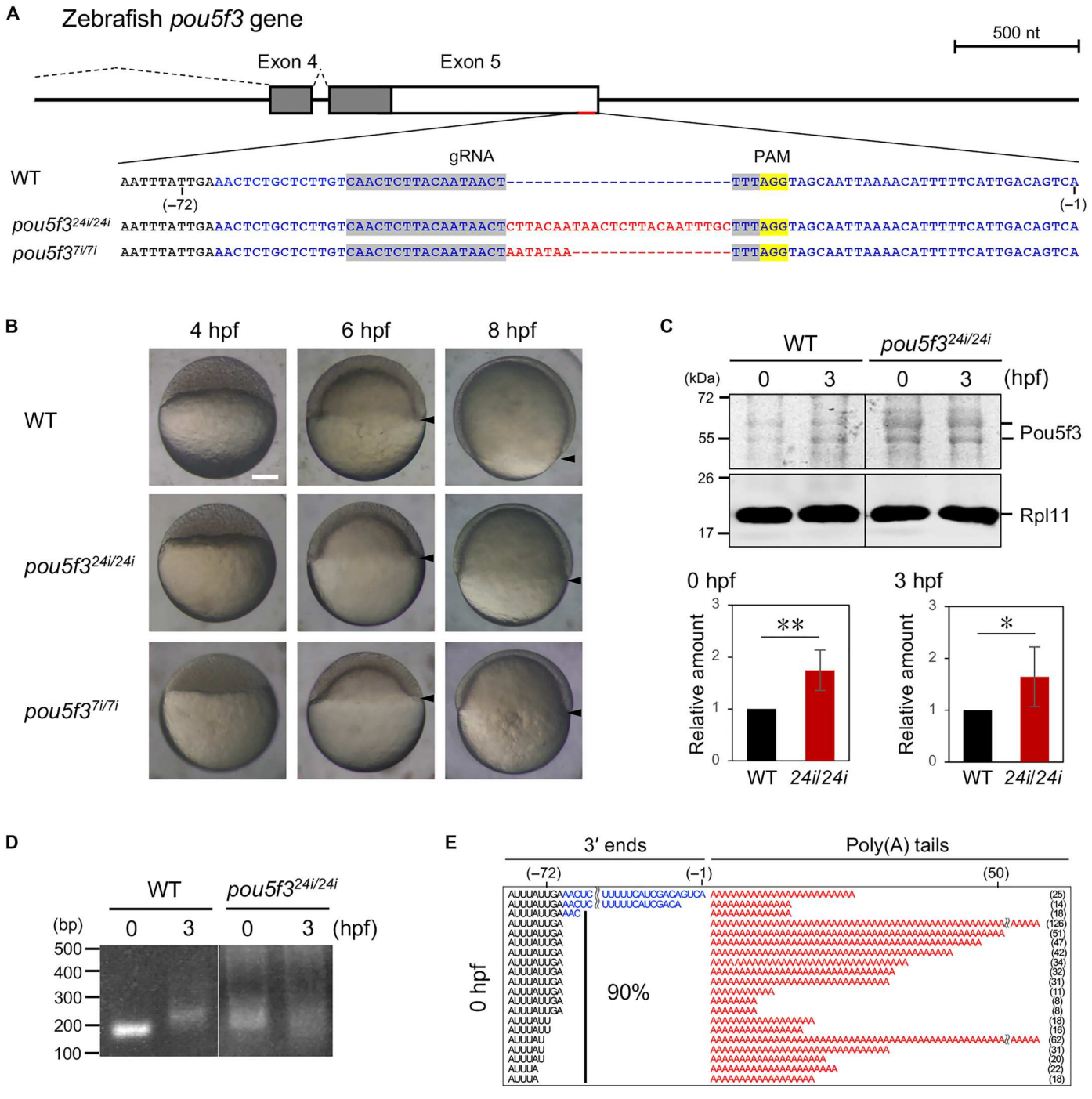

Fig. 4. The 24- and 7-nt insertions at the 3′ end of *pou5f3* cause developmental retardation, increased Pou5f3 accumulation, and precocious 3′ end processing. (**A**) A schematic diagram of *pou5f3* and the 3′ end sequences in the wild-type (WT) and *pou5f3*$^{24i/24i}$ and *pou5f3*$^{7i/7i}$ mutants. Sequences in blue and red denote an additional 3′ end and inserted nucleotides, respectively. Protospacer adjacent motif (PAM) and guide RNA (gRNA) sequences are highlighted in yellow and gray, respectively. (**B**) Lateral views of WT and *pou5f3*$^{24i/24i}$ and *pou5f3*$^{7i/7i}$ mutant embryos at 4, 6, and 8 hpf. Arrowheads indicate the marginal cells, showing the progression of epiboly. *pou5f3*$^{24i/24i}$ and *pou5f3*$^{7i/7i}$ mutant embryos exhibited delayed epiboly progression at 6 and 8 hpf. Similar results were obtained from three independent experiments. Scale bar, 200 μm. (**C**) Top: Immunoblotting of Pou5f3 in WT and *pou5f3*$^{24i/24i}$ embryos at 0 and 3 hpf. Rpl11 is a loading control. Similar results were obtained from five independent experiments. (**C**) Bottom: Intensities of both Pou5f3 bands were quantified (means ± SD; $n = 5$). $^{**}P < 0.01$ and $^{*}P < 0.05$, Student's t test. The intensities of the upper and lower Pou5f3 bands were quantified in fig. S5B. (**D**) PAT assay for zebrafish *pou5f3* mRNA in WT and *pou5f3*$^{24i/24i}$ embryos at 0 and 3 hpf. Similar results were obtained from two independent experiments. (**E**) Sequence analysis of the 3′ ends of *pou5f3* mRNA in *pou5f3*$^{24i/24i}$ embryos at 0 hpf. The lengths of 3′ ends (left) and poly(A) tails (right) are presented.

Unexpectedly, the 24- and 7-nt insertions were removed from *pou5f3* mRNAs carrying long 3′UTRs. Nevertheless, these results suggest that the insertions in the *pou5f3* 3′UTR caused precocious shortening of the 3′ ends and promoted Pou5f3 synthesis in eggs and embryos.

Inhibition of mRNA shortening reduces protein synthesis and affects embryonic development

To explore whether the inhibition of mRNA shortening affects protein synthesis and embryonic development, we injected zebrafish eggs with a morpholino oligonucleotide (MO) that targets the 3′ end of *pou5f3* mRNA (3′end-MO; Fig. 5A). Injection with 3′end-MO, but not control MO containing 5-nt mismatches (5mm-MO; Fig. 5A), caused severe developmental defects, including delayed epiboly, thicker blastoderm during gastrulation (6 and 8 hpf; Fig. 5B), and embryos that were notably shortened along the anterior-posterior axis in the tailbud stage (12 hpf; Fig. 5B). All these defects were consistent with those observed in embryos injected with *pou5f3*-ATG-MO (Fig. 5B), which targets the translation initiation codon (*37*), and mutant embryos lacking maternal and paternal *pou5f3* function (*39*). Immunoblotting revealed that injection with 3′end-MO, but not 5mm-MO, inhibited Pou5f3 protein synthesis (Fig. 5C). The PAT assay failed to detect full-length *pou5f3* mRNA in 3′end-MO–injected embryos, most likely due to RNA-DNA hybrid formation at the 3′ end, which prevents anchor primer ligation. The total amounts of *pou5f3* mRNA and long-type *pou5f3* mRNA were quantified after reverse transcription with random hexamers and a primer complementary to the sequence upstream of the target site of 3′end-MO. Although the total amount of *pou5f3* mRNA remained unchanged, the amount of long *pou5f3* mRNA significantly increased in embryos injected with 3′end-MO (Fig. 5D). These findings emphasize the substantial role of *pou5f3* mRNA translation after fertilization in regulating embryonic development and suggest that shortening of 3′ end sequences directs mRNA translational activation to drive embryonic development.

RNA pull-down assay isolates proteins that bind to long and short *pou5f3* 3′UTRs

Results of reporter assays, genome-edited zebrafish experiments, and embryo injection with MO revealed that the shortening of 3′ end sequences is crucial for the translational activation of *pou5f3* and *Pou5f1* mRNAs. However, the molecular mechanisms underlying the translational regulation of these mRNAs remain unknown. To gain an insight into the molecular mechanisms of *pou5f3* and *Pou5f1* mRNA translation through 3′ end shortening, we isolated proteins specifically binding to the long and/or short 3′UTRs of *pou5f3* mRNA using in vitro–synthesized RNAs and zebrafish oocyte extracts. This is because sufficient materials were obtained using zebrafish oocytes, but not using mouse oocytes. The

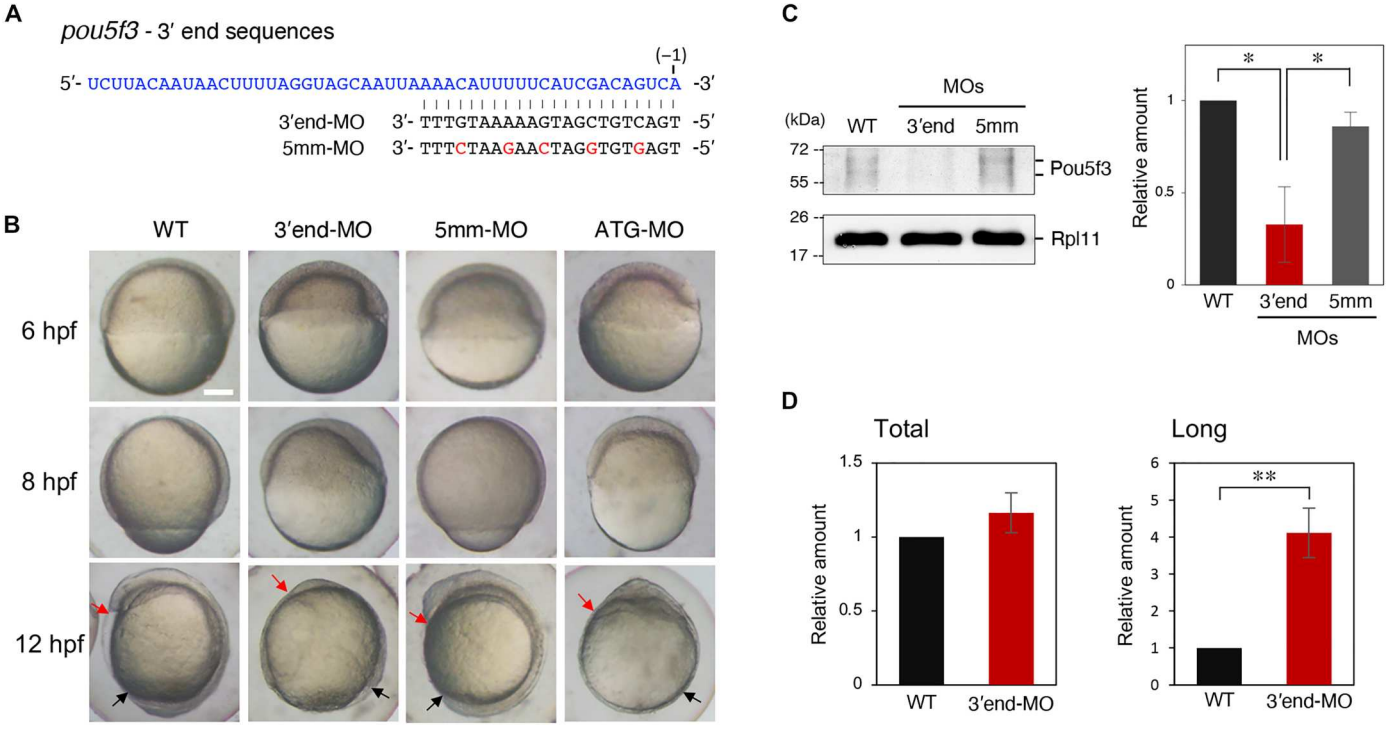

Fig. 5. Injection with MO targeting 3′ end sequences of *pou5f3* prevents Pou5f3 accumulation and causes severe developmental defects. (**A**) 3′ end sequences of *pou5f3* mRNA that are targeted by 3′end-MO. 5mm-MO contains five mismatches (red). (**B**) Lateral views of WT and 3′end-MO–, 5mm-MO–, or ATG-MO–injected embryos at 6, 8, and 12 hpf. The 3′end-MO–injected embryos exhibited defective gastrulation (thickened blastoderm and delay in epiboly progression) and shortened anterior-posterior axis (red and black arrows). Similar results were obtained from the three independent experiments. Scale bar, 200 μm. (**C**) Immunoblotting of Pou5f3 in embryos injected with 3′end- or 5mm-MO at 4 hpf (left). The intensities of both Pou5f3 bands were quantified (means ± SD; $n = 3$) (right). *$P < 0.05$, Tukey's multiple comparison test. (**D**) Levels of total *pou5f3* mRNA (Total) and long *pou5f3* mRNA (Long) in WT embryos and embryos injected with 3′end-MO at 4 hpf were determined by quantitative RT-PCR (means ± SD; $n = 3$). **$P < 0.01$, Student's t test.

sequences of the 100-terminal nucleotides of zebrafish *pou5f3* and mouse *Pou5f1* mRNAs shared 43.1% identity (fig. S6). Thus, it is likely that both mRNAs bind to similar proteins. Proteins coprecipitated with a long or short *pou5f3* 3′UTR or an antisense strand of long *pou5f3* 3′UTR were purified and analyzed by mass spectrometry (Fig. 6A). We first categorized proteins that bound to long 3′UTR alone as long-specific proteins. Similarly, proteins that bound to short 3′UTR alone were categorized as short-specific proteins. Second, proteins that bound to both 3′UTR types were categorized as follows. When the number of peptides isolated with long 3′UTR was twofold higher than that of peptides isolated with short 3′UTR, these proteins were categorized as long-specific proteins. Short-specific proteins were categorized similarly. The remaining proteins were categorized as proteins binding to both 3′UTR types after removing nonspecific bounds, i.e., when the number of peptides in all precipitations was equivalent. Last, 129 proteins were isolated as proteins specifically binding to the long-type *pou5f3* 3′UTR, 191 proteins specifically binding to the short-

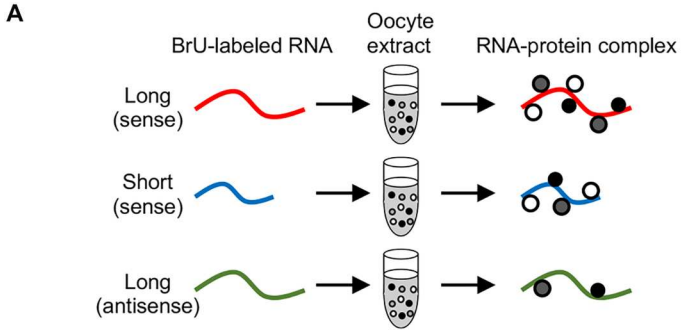

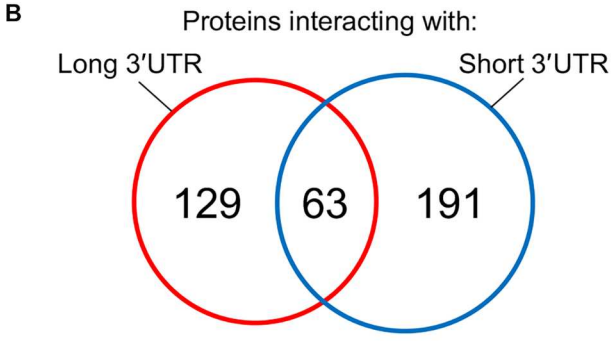

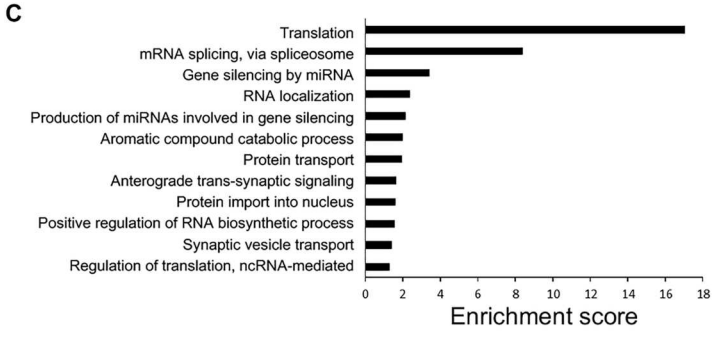

D

	Gene	Peptide counts Long	Short
Long and Short	HuB	75	56
	HuR	16	10
	CPEB1	7	9
Long	hnRNP D	14	4
Short	Gemin5	3	22
	Dhx9	3	23
	CPSF1	0	1
	Pabpc1l	13	28

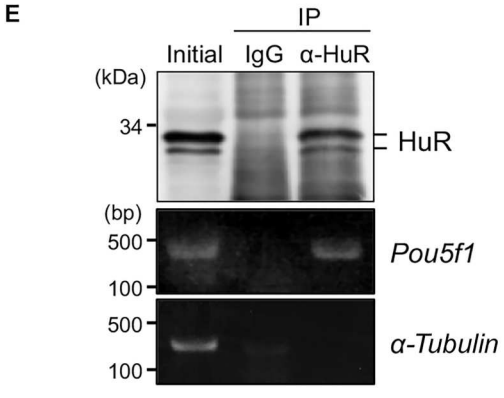

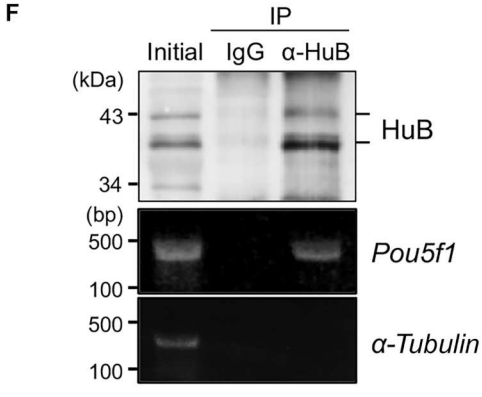

Fig. 6. Isolation of proteins binding to the long and/or short *pou5f3* 3′UTRs. (**A**) A schematic diagram of the isolation of proteins specifically binding to in vitro–synthesized *pou5f3* long or short sense RNAs or long antisense RNA. (**B**) Venn diagram depicts the number of proteins isolated as proteins interacting with long (red) and short (blue) 3′UTR sequences of *pou5f3* and the number of proteins binding to both 3′UTRs. (**C**) GO analysis of genes enriched in proteins isolated as proteins interacting with *pou5f3* 3′UTR sequences. (**D**) Representations of proteins isolated in the RNA pull-down assay. (**E** and **F**) IP/RT-PCR analysis of HuR and HuB with *Pou5f1* mRNA. Top: Immunoblotting of mouse ovary extracts before IP (initial) and IP with control immunoglobulin G (IgG) or anti-HuR (α-HuR) (E) and anti-HuB (α-HuB) (F) antibodies. Bottom: Semiquantitative RT-PCR amplification of *Pou5f1* and α-*tubulin* transcripts. Similar results were obtained from two independent experiments. BrU, bromouridine; ncRNA, noncoding RNA.

type *pou5f3* 3′UTR, and 63 proteins binding to both long and short *pou5f3* 3′UTRs (Fig. 6B and table S1). The Gene Ontology (GO) terms of these proteins were associated with translation and mRNA splicing (Fig. 6C).

To validate the results of the RNA pull-down assay, we analyzed the interactions between endogenous proteins and mRNAs by immunoprecipitation followed by RT-PCR (IP/RT-PCR). HuR and HuB were isolated as proteins binding both long and short *pou5f3* 3′UTRs (Fig. 6D and table S1), and previous studies have revealed their expression in mouse ovaries (*48*). *Pou5f1* mRNA was detected in the precipitates of anti-HuR and anti-HuB antibodies but not in those of control immunoglobulin G (IgG) (Fig. 6, E and F). These results demonstrated that the findings of the RNA pull-down assay reflect in vivo interactions.

Heterogeneous nuclear ribonucleoprotein D (hnRNP D), Gemin5, and DEAH-box polypeptide 9 (Dhx9) regulate *Pou5f1* mRNA translation

To determine the molecular mechanisms of translational regulation through the shortening of 3′ end sequences, we focused on RNA binding proteins that predominantly interacted with long or short *pou5f3* 3′UTR (Fig. 6D and table S1). We focused on hnRNP D as a protein binding to long 3′UTR and Gemin5 and Dhx9 as proteins binding to short 3′UTR (Fig. 6D). We used mouse oocytes and embryos because this system is applicable to cell biological and functional analyses of proteins stored in oocytes (*31*, *32*, *49*).

hnRNP D, a member of the hnRNP family RNA binding proteins, has been demonstrated to participate in RNA splicing and regulation of RNA stability and translation (*50*). First, we analyzed the mRNA and protein expression in fully grown mouse oocytes. RT-PCR and immunoblotting revealed the *hnRNP D* mRNA and hnRNP D protein expression in mouse oocytes (fig. S7, A and B). Immunofluorescence analysis of oocytes indicated that hnRNP D was distributed in the cytoplasm and in the oocyte nucleus, germinal vesicle (Fig. 7A). The interaction of hnRNP D with *Pou5f1* mRNA was confirmed by IP/RT-PCR (Fig. 7B). Together, these results suggest that *Pou5f1* mRNA is a target of hnRNP D in mouse oocytes.

To elucidate whether hnRNP D plays a role in *Pou5f1* mRNA regulation, we knocked down hnRNP D using the Trim-Away protein degradation system with anti–hnRNP D antibody. This system allows the degradation of an endogenous protein by Tripartite motif-containing protein (TRIM)-mediated degradation of the antibody-target protein complex (*49*). We injected immature oocytes with *Trim21* mRNA and anti–hnRNP D antibody and incubated them with M2+ medium for 16 hours. As shown in Fig. 7C, hnRNP D was efficiently degraded by the degradation system. Next, we knocked down hnRNP D in one-cell stage embryos and observed the expression of Pou5f1 in early two-cell stage embryos. Immunofluorescence analysis revealed an increase in Pou5f1 expression in the early two-cell stage embryos (Fig. 7D). These results suggest that hnRNP D represses *Pou5f1* mRNA translation in early-stage mouse embryos.

Gemin5 is an RNA binding protein of the survival motor neuron (SMN) complex, which plays a critical role in splicing. It is also a regulator of cap-dependent and cap-independent translation (*51*, *52*). Dhx9 (also known as RNA helicase A), a member of the DEAD box RNA helicase family proteins, plays important roles in various cellular processes, including transcription, splicing, and translation (*53*). To determine whether Gemin5 and Dhx9 participate in *Pou5f1* mRNA translation, we first analyzed their expression in fully grown mouse oocytes. RT-PCR and immunoblotting confirmed the expression of *Gemin5* and *Dhx9* mRNAs and Gemin5 and Dhx9 proteins in mouse oocytes (fig. S7, A and B). Immunofluorescence revealed the expression of Gemin5 in the cytoplasm of oocytes and two-cell stage embryos (Fig. 7A). In addition to its cytoplasmic distribution, Gemin5 was localized around the chromosome of mature oocytes and in the nucleus of two-cell stage embryos. Immunofluorescence analysis demonstrated the high expression of Dhx9 in the nucleus of oocytes and two-cell stage embryos and low expression of Dhx9 in the cytoplasm (Fig. 7A). The RNA pull-down assay revealed that Gemin5 interacted with in vitro–synthesized RNAs consisting of mouse *Pou5f1* 3′UTRs (fig. S7C). Consistent with the mass spectrometry results, Gemin5 interacted more strongly with short *Pou5f1* than with long *Pou5f1* (fig. S7D). In addition, using an ultraviolet (UV)–crosslinking assay, the interactions of Gemin5 and Dhx9 with *Pou5f1* mRNA were confirmed by reactions between immunoprecipitated Gemin5 and Dhx9 proteins and in vitro–synthesized RNAs consisting of the short *Pou5f1* 3′UTR (fig. S7E). IP/RT-PCR in early two-cell stage embryos revealed that Gemin5 and Dhx9 interacted with *Pou5f1* mRNA (Fig. 7B). As most *Pou5f1* mRNAs were shortened at this stage (Fig. 1E), Gemin5 and Dhx9 may bind to short-type *Pou5f1* in embryos.

Subsequently, we knocked down Gemin5 and Dhx9 using the Trim-Away protein degradation system with anti-Gemin5 and anti-Dhx9 antibodies. As presented in Fig. 7C, Gemin5 and Dhx9 were effectively degraded by this degradation system. The translational efficiency of the reporter mRNA in mature oocytes was initially investigated by injecting the 14-nt-deleted *Pou5f1* mRNA (fig. S8A). Dhx9 knockdown significantly reduced the translational activation of reporter mRNA in mature oocytes, whereas Gemin5 knockdown slightly reduced the translation, with no significant difference (fig. S8B), indicating that Dhx9 is required for the translational activation of short *Pou5f1* mRNA in mature oocytes. Next, we examined the synthesis of endogenous Pou5f1 by immunofluorescence. Gemin5 and Dhx9 knockdown in one-cell stage embryos led to significantly reduced Pou5f1 expression in the early two-cell stage embryos (Fig. 7E). The Trim-Away system did not affect the level of *Pou5f1* mRNAs and shortening of their 3′ ends in the early two-cell stage embryos (fig. S8, C to E). Therefore, these results suggest that shortened *Pou5f1* mRNA is translationally activated via the binding of Gemin5 and Dhx9 during the cleavage stage.

The 3′ ends of a diverse group of mRNAs are shortened after fertilization

We lastly elucidated whether the mature mRNA processing is unique to a subset of mRNAs or a general process in global mRNAs. Accordingly, we performed 3′ end RNA sequencing in which the 3′ end fragments of mRNAs containing poly(A) tails were reverse-transcribed with an oligo(dT) primer, and sequences close to the 3′ ends of the transcripts were obtained using zebrafish embryos at 0 and 4 hpf (Fig. 8A). The resultant sequences were mapped onto the zebrafish genome (ensemble v11). This assay enabled the detection of the 3′ ends of distinct mRNAs. For example, all reads of *tktb* and *pycr1b* mRNAs were mapped onto the end of the last exon in embryos at 0 and 4 hpf (Fig. 8B), indicating that the 3′ end of these mRNAs was not altered during this

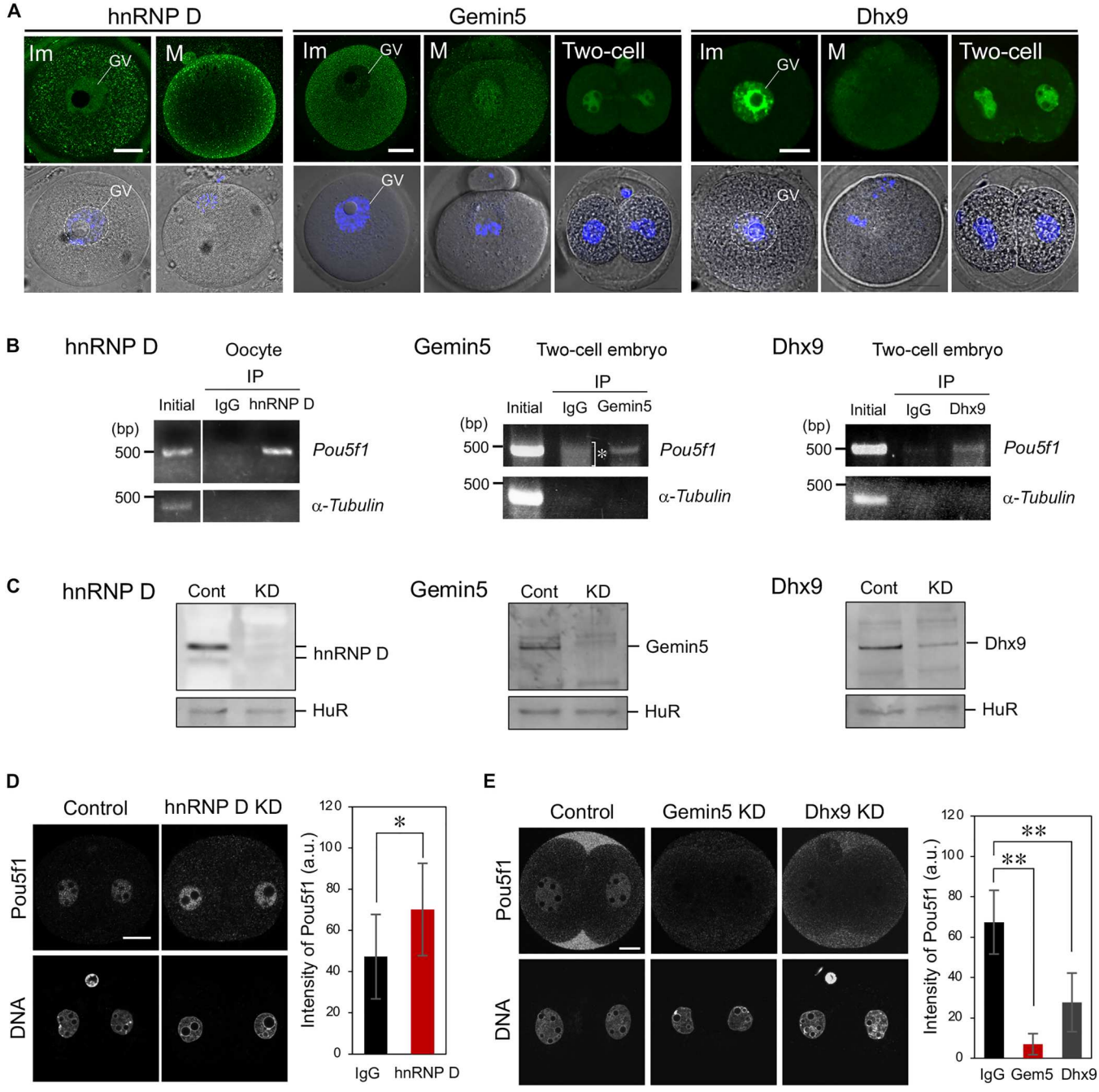

Fig. 7. hnRNP D, Gemin5, and Dhx9 regulate the translation of *Pou5f1* mRNA in mouse embryos. (**A**) Immunofluorescence of hnRNP D, Gemin5, and Dhx9 in mouse immature (Im) and mature (M) oocytes and two-cell stage embryos (Two-cell). GV, germinal vesicle. (**B**) IP/RT-PCR analysis of hnRNP D (left), Gemin5 (middle), and Dhx9 (right) with *Pou5f1* mRNA. Left: Semiquantitative RT-PCR amplification of *Pou5f1* and *α-tubulin* transcripts of mouse ovary extracts before IP (initial) and IP with control IgG (IgG) or anti–hnRNP D (hnRNP D) antibody. Similar results were obtained from three independent experiments. Middle and Right: Semiquantitative RT-PCR amplification of *Pou5f1* and α-tubulin transcripts of mouse two-cell stage embryos before IP (initial) and IP with control IgG (IgG) or anti-Gemin5 (Gemin5) or anti-Dhx9 (Dhx9) antibody. An asterisk indicates nonspecific amplifications. (**C**) Immunoblotting of oocytes injected without [control (Cont)] or with anti–hnRNP D (left), anti-Gemin5 (middle), or anti-Dhx9 (right) antibody and *Trim21* mRNA [knockdown (KD)]. (**D**) Left: Immunofluorescence of Pou5f1 in embryos injected with IgG (control) or anti–hnRNP D antibody (hnRNP D KD). DNA is indicated at the bottom. Similar results were obtained from three independent experiments. Right: Intensities of Pou5f1 signals were quantified (means ± SD). a.u., arbitrary unit. *$P < 0.05$, Student's *t* test. (**E**) Left: Immunofluorescence of Pou5f1 in embryos injected with IgG (control) or anti-Gemin5 (Gemin5 KD) and anti-Dhx9 (Dhx9 KD) antibodies. Similar results were obtained from three independent experiments. Right: The intensities of Pou5f1 signals were quantified (means ± SD). **$P < 0.01$, Dunnett's test. Scale bars, 20 μm.

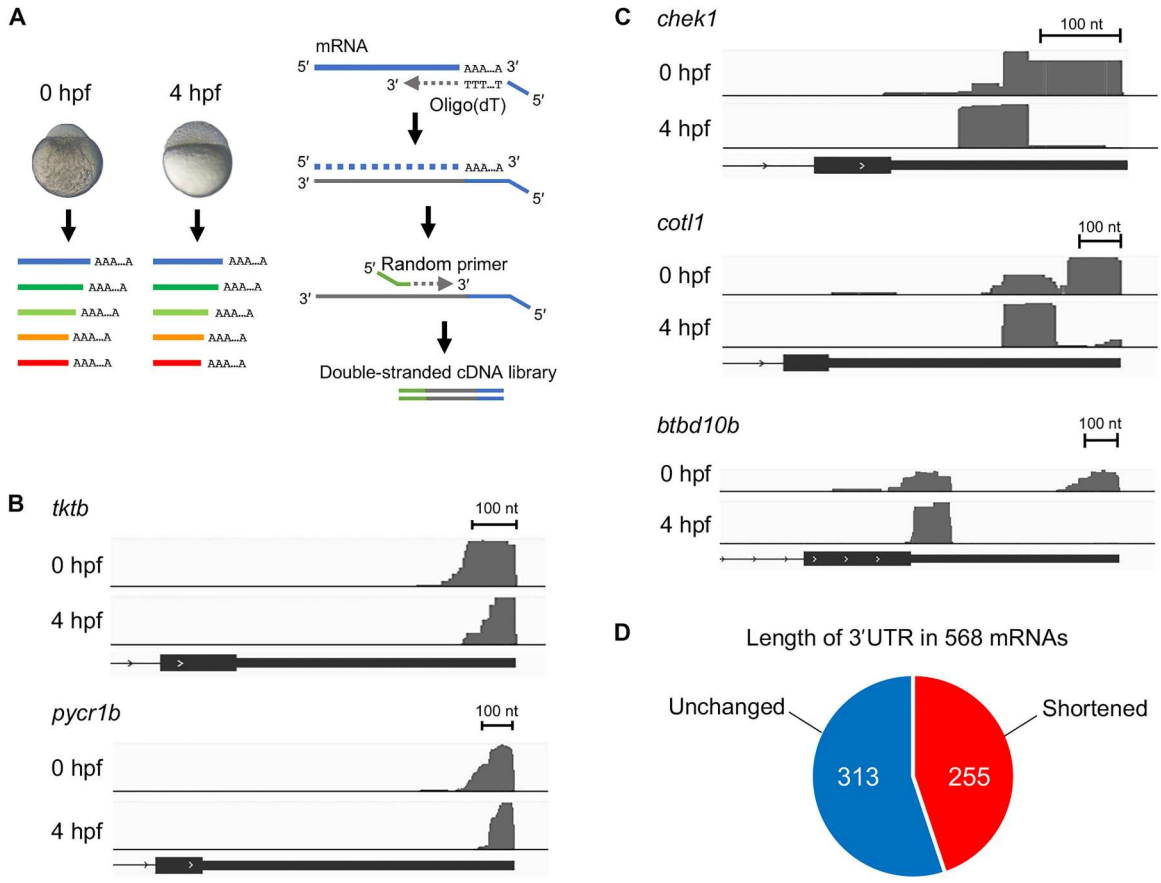

Fig. 8. The 3′ end sequences of a diverse group of mRNAs are shortened during the early development of zebrafish. (**A**) A schematic diagram of the detection of mRNA 3′ ends by 3′ end RNA sequencing. Left: Zebrafish embryos at 0 and 4 hpf were collected and extracted for RNA purification. Right: Total RNAs were reverse-transcribed using an oligo(dT) primer. After removing the RNA template, second-strand DNAs were synthesized by random priming. (**B**) Tracks of 3′ end RNA sequencing plotted on the 3′ genomic region of *tktb* and *pycr1b* from embryos at 0 and 4 hpf. The terminal exon is presented. The numbers of reads were 1062 (0 hpf) and 1372 (4 hpf) in *tktb* and 4392 (0 hpf) and 12378 (4 hpf) in *pycr1b*. (**C**) Tracks of 3′ end sequencing plotted on the 3′ genomic region of *chek1*, *cotl1*, and *btbd10b* from embryos at 0 and 4 hpf. The total numbers of reads were 505 (0 hpf) and 361 (4 hpf) in *chek1*, 17 (0 hpf) and 44 (4 hpf) in *cotl1*, and 809 (0 hpf) and 1217 (4 hpf) in *btbd10b*. The details with *P* values are shown in table S2. (**D**) Summary of 3′ end RNA sequencing of 568 genes with the number of mRNAs with shortened (red) and unchanged (blue) 3′ end between 0 and 4 hpf.

period. Regarding *chek1* mRNA, almost all reads were mapped onto the 3′ end of the last exon at 0 hpf, whereas all reads were mapped approximately 100 nt upstream of the 3′ end at 4 hpf (Fig. 8C). Regarding *cotl1*, most reads were mapped onto the 3′ end of the last exon, but some were mapped approximately 150 nt upstream of the 3′ end at 0 hpf. At 4 hpf, almost all reads were mapped onto the upstream region (Fig. 8C). The 3′ end of *btbd10b* mRNA was similarly changed (Fig. 8C). To accurately examine changes in mRNA 3′ ends, we counted the reads defined as long and short 3′ ends and calculated their proportion (table S2). In the case of *pou5f3* mRNA, 78.8% of mRNAs (total 3342) harbored the long 3′ end at 0 hpf, which decreased to 39.9% (total 4589) at 4 hpf (fig. S9), consistent with the reduction observed in the PAT assay. In total, we analyzed 568 mRNAs, an estimated 5% of the mRNAs demonstrated to be expressed in eggs (*17*) and revealed that 255 mRNAs (44.9%) harbored longer 3′ end sequences in embryos at 0 hpf that were shortened at 4 hpf (Fig. 8D and table S2). These results suggest that the 3′ end sequences of a diverse group of mRNAs are processed after fertilization.

DISCUSSION

RNA processing of the 3′ end sequences of mature mRNAs directs translational activation

After the completion of nuclear RNA processing, the sequences of eukaryotic protein-coding mRNAs are believed to remain unchanged, excluding poly(A) tails, which are shortened by deadenylases and elongated by poly(A) polymerases (*54*). In this study, we demonstrated that the 3′ end sequences of mature mRNAs were processed at a certain length, and poly(A) tails were then added to their 3′ ends (Figs. 1 and 8 and figs. S1 and S3). In general, the removal of the poly(A) tails of mature mRNAs has been demonstrated to promote mRNA degradation (*55*–*57*), which is also observed in the early development of zebrafish and in oocyte maturation of mice (*58*, *59*). However, the total levels of *pou5f3* and *Pou5f1* mRNAs did not decrease after the shortening most mRNAs (Fig. 1 and fig. S1) (*36*). Marked increases in zygotic transcript levels during this period were unlikely because only a small number of zygotic mRNAs were detected in zebrafish at ~4 hpf, and transcription was demonstrated to begin after the late two-cell stage

in mice (fig. S2) (*7*, *11*). Therefore, our results indicate that this RNA processing is not coupled with mRNA degradation. Conversely, four independent lines of evidence illustrated that this RNA processing promotes the translational efficiency of mRNAs. First, analyses of transgenes in zebrafish demonstrated that the reporter mRNA with a shortened 3′UTR, but not a full-length 3′UTR, was effectively translated in early development (Fig. 2). Second, reporter assays in mice demonstrated that shortening of the 3′UTR increased the translational efficiency in mature oocytes (Fig. 3). Third, genome editing in zebrafish demonstrated that the precocious shortening of 3′UTR promoted the translational activation of *pou5f3* mRNA in eggs (Fig. 4). Fourth, inhibition of mRNA shortening by MO injection prevented Pou5f3 accumulation (Fig. 5). Collectively, our results uncovered a previously unknown RNA processing that triggers the translational activation of mRNAs stored in a dormant state.

Our sequence analyses of *pou5f3* and *wnt8a* mRNAs in zebrafish and *Pou5f1* mRNA in mice showed that the deletion of 3′ end nucleotides had detectable patterns (Fig. 1 and fig. S3). In addition, poly(A) tails appeared to be transiently shortened before or consistently with the 3′ end deletion (Fig. 1 and figs. S1 and S3). For example, zebrafish *pou5f3* mRNA was shortened by 68 or 72 nt in almost all cases, and the poly(A) tails were elongated in mRNAs harboring the shortened 3′ ends (Fig. 1B and fig. S1B). Although the 9-nt deletion was abundant in mouse *Pou5f1* mRNA, the number of nucleotides showed a gradual change (Fig. 1E). The poly(A) tails were once shortened in mature oocytes and elongated again in two-cell stage embryos (Fig. 1, E and F). A possible explanation for this finding is that a deadenylase first removes poly(A) tails, after which 3′ end sequences are deleted by an exonuclease. Another possibility is that deadenylases shorten the 3′ end sequences after removing poly(A) tails, as some deadenylases can delete nucleotides other than polyadenine (*60*, *61*). Further studies are warranted to isolate enzymes mediating the deletion of 3′ end sequences.

Although the importance of polyadenylation after 3′ end processing remains obscure, several findings suggest that this process is crucial to the translational activation of shortened mRNAs. First, after shortening of the 3′ ends at the time of translation, all mRNAs examined in this study had poly(A) tails (Figs. 1 and 4 and figs. S3 and S5). Second, the reporter mRNA with a long *pou5f3* 3′UTR was shortened, and poly(A) tails were inserted in zebrafish embryos at 4 hpf (fig. S4C). Third, in mature mouse oocytes, the reporter mRNA with a short *Pou5f1* 3′UTR, but not long *Pou5f1* 3′UTR, was polyadenylated (fig. S4E). Furthermore, previous studies have demonstrated that the inhibition of polyadenylation causes severe defects in the early development of zebrafish (*5*, *17*). As poly(A) tails of long *pou5f3* mRNA were once elongated in fertilized eggs, likely due to high activities of poly(A) polymerases, but were not translationally activated (fig. S1) (*37*), polyadenylation after the shortening of 3′ ends may be a substantial process for the translational activation after fertilization.

Our sequence analyses also illustrated that mature mRNA processing begins at different developmental stages of zebrafish and mouse. For example, the proportion of *pou5f3* mRNA carrying shortened 3′ ends substantially increased during the mitotic cleavage stage in zebrafish (Fig. 1B), whereas that of *Pou5f1* mRNA carrying shortened 3′ ends increased during oocyte maturation in mice (Fig. 1E). These differences are consistent with those observed in mRNA degradation in zebrafish and mouse development. The first wave of mRNA degradation begins shortly after fertilization in zebrafish (*58*), whereas it begins during oocyte maturation in mice (*62*). These findings suggest that molecular events occur in earlier stages in mice than in zebrafish.

Changes in the 3′UTR length of mRNAs via alternative polyadenylation (APA) have been reported during embryonic development in mice and zebrafish (*63*, *64*). APA arises from differences in the selection of pre-mRNA 3′ cleavage sites by an endonuclease, followed by the addition of a poly(A) tail. Systematic analyses of APA have demonstrated an increase in the lengths of 3′UTRs in numerous mRNAs during developmental progression after ZGA. In this study, 3′ end RNA sequencing revealed the shortening of 3′ ends in a diverse group of mRNAs at 4 hpf (Fig. 8), which is contradictory to the lengthening of the 3′UTRs of zygotic transcripts by APA. These differences support the notion that maternally deposited mRNAs are globally shortened after fertilization.

Mature mRNA processing drives embryonic development

An unexpected finding in our mutant zebrafish was that the 24- and 7-nt insertions in the 3′ end sequences were removed from mature *pou5f3* mRNAs carrying full-length 3′UTRs (Fig. 4 and fig. S5). A possible explanation for this finding is that the insertions are deleted from pre-mRNAs via splicing. Ectopic splicing may alter the composition of proteins binding to the 3′ end sequences because it affects the subsequent binding of RNA binding proteins to mRNAs that are important for the cytoplasmic regulation (*50*). Ectopic splicing may inhibit the binding of a protein that protects mRNA from 3′ end processing or recruit a protein to the mRNA that promotes 3′ end shortening. Although the precise mechanisms remain to be addressed, this insertion caused precocious shortening of 3′ end sequences, resulting in Pou5f3 protein synthesis and developmental retardation (Fig. 4 and fig. S5).

In mice, overexpressing Pou5f1/Oct4 by injecting *Pou5f1*/*Oct4* mRNA into one-cell stage embryos caused developmental arrest in early cleavage stages, with inappropriate induction of gene expression (*65*, *66*). The genome-edited zebrafish experiments illustrated that increased Pou5f3 expression retarded the progression of gastrulation (Fig. 4B), indicating that Pou5f3 up-regulation similarly affects development, although this effect appears mild compared with that in mice. In the immunoblot analysis, the amount of the upper band of Pou5f3, which was confirmed to be a phosphorylated form of Pou5f3 (*43*), was significantly increased in *pou5f3*$^{24i/24i}$ and *pou5f3*$^{7i/7i}$ eggs and embryos (Fig. 4C and fig. S5, B to D). Although the functional differences between the two types of Pou5f3 remain unknown, it is possible that phosphorylation attenuates the Pou5f3 function, as observed in the case of Pou5f1/Oct4 oxidation in human embryonic stem (ES) cells (*67*). Nevertheless, our results indicate that defective translation repression of endogenous *pou5f3* mRNA causes abnormal progression of early development.

In contrast to the results of genome editing, injection with MO targeting the 3′ end sequences of *pou5f3* mRNA prevented 3′ end shortening and Pou5f3 synthesis (Fig. 5, A, C, and D). These findings support the notion that an exonuclease removes the 3′ end sequences, allowing mRNA translation. Translational inhibition of *pou5f3* mRNA resulted in severe developmental defects (Fig. 5B), which were consistent with the defects observed in maternal and paternal *pou5f3* mutants (*38*–*42*). Collectively, our findings

demonstrate that the translational state of *pou5f3* mRNA is temporally regulated during the early stages of development by the presence and shortening of 3′ end sequences to accurately regulate Pou5f3 expression, which is crucial for driving embryonic development.

Shortening of 3′ ends after fertilization acts as molecular switches

Since the earliest findings of translational regulation in sea urchin eggs in the 1960s, the mechanisms underlying the temporal regulation of mRNA translation have been extensively studied during oocyte maturation in *Xenopus* oocytes. In particular, polyadenylation-mediated translational regulation has been well studied using *cyclin B1* mRNA, which encodes a regulatory subunit of maturation/M phase–promoting factor. In immature *Xenopus* oocytes, both the Poly(A)-specific ribonuclease (PARN) and poly(A) polymerase GLD2 bind to the 3′UTR of *cyclin B1* mRNA (*68*). The high activity of PARN causes the shortening of the poly(A) tail of *cyclin B1* mRNA. After the initiation of oocyte maturation, cytoplasmic polyadenylation element (CPE)–binding protein (CPEB), which binds to the CPEs of *cyclin B1* mRNA, is phosphorylated (*69*). Phosphorylated CPEBs recruit cleavage and polyadenylation specificity factor (CPSF) to the polyadenylation signal in the 3′UTR of mRNA, promoting the exclusion of PARN from the mRNA and facilitating GLD2-mediated polyadenylation. A long poly(A) tail serves as a binding site for poly(A)–binding protein (PABP), which cooperates with the eukaryotic translation initiation factor 4G (eIF4G) and cap-binding protein eIF4E to promote translation (*70*).

Consistent with the model of translational regulation in oocyte maturation, we isolated CPEB1 as a protein that binds to both long and short 3′UTRs of *pou5f3* mRNA in the RNA pull-down assay (Fig. 6D and table S1). Further, we isolated CPSF1 and the PABP Pabpc1l as proteins that mainly bind to the short 3′UTR (Fig. 6D and table S1). Although future studies are warranted to determine whether these factors are involved in translational regulation after fertilization, our results suggest that, at least in part, the translation of mRNAs stored in eggs is regulated in a manner similar to that in oocyte maturation.

In this study, we unveiled the molecular mechanisms of mRNA translation through the shortening of 3′ end sequences. The 9-nt mutations in the 3′ end sequences of *Pou5f1* mRNA alleviated the translational repression of reporter mRNAs in immature mouse oocytes (Fig. 3E), suggesting the existence of a trans-acting factor that represses mRNA translation. In addition, we isolated hnRNP D as a protein that binds to unprocessed *pou5f3* 3′UTR in vitro and confirmed its binding to *Pou5f1* mRNA in vivo (Figs. 6 and 7B). hnRNP D knockdown increased the accumulation of Pou5f1 in the nuclei of two-cell stage embryos (Fig. 7D). hnRNP D is known to bind to the 5′ and 3′UTRs of target mRNAs and affect their splicing, stability, and translation (*71*, *72*). These results suggest that hnRNP D represses *Pou5f1* mRNA translation, although its binding sequences remain unidentified, and support the notion that *Pou5f1* mRNA translation is repressed by factors that bind to its 3′UTR. A possible scenario is that one or more factors protect 3′ ends from processing. Further, we isolated Gemin5 and Dhx9 as proteins that bind to the processed 3′UTRs of *Pou5f1* mRNA and are required for Pou5f1 accumulation (Figs. 6 and 7). Gemin5 targets several mRNAs and regulates their translation, including the translational activation of SMN mRNA (*52*, *73*). Dhx9 plays a role in various mRNA regulatory processes, including the translation of selected mRNAs in mammalian cells and *Pou5f1*/*Oct4* mRNA in human ES cells (*74*, *75*). Both Gemin5 and Dhx9 have been demonstrated to recruit ribosomes to promote translation of selective mRNAs, possibly in the same complex (*75*, *76*). Although Dhx9 target sites remain unknown, Gemin5 targets the specific sequence AUUUUU in both pre- and mature mRNAs (*51*, *73*). *pou5f3* and *Pou5f1* mRNAs contain Gemin5 target sites in their processed 3′UTRs. Together, Gemin5 and Dhx9 can bind to the 3′UTRs of *pou5f3* and *Pou5f1* mRNAs after 3′ end processing and recruit ribosomes to promote their translation. However, we could not rule out the possibility that Gemin5 and Dhx9 modifications promote the translation rate after binding to the *Pou5f1* 3′UTR. Further detailed analyses should be performed in future studies.

HuR and HuB were demonstrated to bind to the *pou5f3* 3′UTR in vitro and *Pou5f1* mRNA in vivo (Fig. 6). These proteins are known as components of stress granules, which are assemblies of mRNA and RNA binding proteins (*48*). The results of the RNA pull-down assay suggested that the binding of HuR and HuB to *pou5f3* mRNA persists after the shortening of mRNA. As HuR knockdown reduces the sizes of granules in cultured cells (*77*), this protein might function as a core of the RNA binding protein assemblies in both unprocessed and processed mRNAs. The RNA pull-down assay suggested that long and short *pou5f3* mRNAs share a certain number of proteins, but many proteins are altered after shortening (Fig. 6), although the validity of these alterations in vivo remains unexplored. The secondary structures of *pou5f3* and *Pou5f1* may have been altered after the 3′ end shortening, which might explain the alterations in binding proteins (fig. S10A and B). An RNA helicase, such as Dhx9, could also remodel the mRNA structure (*53*). In mouse oocytes, the reporter assay revealed that Dhx9, but not Gemin5, is required for the translational activation of reporter mRNA with a short *Pou5f1* 3′UTR in mature oocytes (fig. S8, A and B). Considering that the translation rate of endogenous *Pou5f1* mRNA gradually increases until the early two-cell stage (*36*), Dhx9 may alter the secondary structure of mRNA as a first step, resulting in the recruitment of other proteins, such as Gemin5, which are crucial for promoting translation in later stages (Fig. 7). As other RNA helicases tend to bind to the short 3′UTR (table S1), the secondary structure of mRNA could be remodeled gradually, potentially increasing the binding protein levels and translational efficiency. Additionally, the reporter assay in mise revealed differences in translation rates between the reporter mRNA with mutations at the 3′ end (Fig. 3, D and E). This might be due to variations in the secondary structures of the 2m-, 5m-, and 9m-reporter mRNAs (fig. S10C). The 9-nt mutation, in particular, could lead to a large structural change at the 3′ end, which may result in partial derepression of translation in immature oocytes. The compositional changes in *pou5f3* mRNA may be linked to changes in the physical properties of *pou5f3* embryonic RNA granules from solid-like to liquid-like, which has been shown to promote translational efficiency (*37*). Proteins binding to short-type mRNA may sustain the solid-like state of granules, whereas those binding to long-type mRNA may accelerate the phase change into a liquid-like state, thereby effectively promoting a translational state in membrane-less compartments.

The finding that zebrafish eggs can promote translation of shortened *pou5f3* mRNAs suggest that the mRNA translation is strictly

repressed in this stage via 3′ end sequences. The identification of the molecular events that initiate 3′ end shortening is a critical issue that must be addressed in future investigations. As hnRNP D, Gemin5, and Dhx9 target a wide range of mRNAs, they could potentially regulate the translation of other selective mRNAs. It remains unclear whether these proteins regulate the translation of the mRNAs that had been shortened after fertilization in 3′ end RNA sequencing.

Our study provides a key molecular principle of mRNA translation after fertilization, which has remained unresolved for decades after finding the accumulation of dormant mRNAs in eggs. These discoveries should facilitate studies on the mechanisms of promoting early development and may contribute to understanding the temporal regulation of mRNA translation in diverse cellular and developmental processes.

MATERIALS AND METHODS

Collection of oocytes and embryos

All animal experiments in this study were approved by the Committee on Animal Experimentation, Hokkaido University (license number 20-0135). AB and Tübingen zebrafish were maintained at 28°C on a 14-hour light/10-hour dark cycle following standard methods. Zebrafish oocytes were manually isolated from ovaries in zebrafish Ringer′s solution (116 mM NaCl, 2.9 mM KCl, 1.8 mM $CaCl_2$, and 5 mM Hepes; pH 7.2) using forceps under a dissecting microscope. Oocyte maturation was induced by treatment with 17α, 20β-dihydroxy-4-pregnen-3-one (1 μg/ml), a maturation-inducing hormone in fish. Embryos were obtained via natural spawning and staged according to the time post fertilization and morphological criteria. To inhibit zygotic transcription, 50 ng of amanitin was injected into fertilized eggs. For the PAT assay, oocytes and embryos were extracted with TRIzol reagent (Invitrogen), and total RNA was used for RNA ligation–coupled RT-PCR. For immunoblotting, embryos were homogenized with an equal volume of ice-cold extraction buffer [EB; 100 mM β-glycerophosphate, 20 mM Hepes, 15 mM $MgCl_2$, 5 mM EGTA, 1 mM dithiothreitol, 100 μM (*p*-amidinophenyl) methanesulfonyl fluoride, and leupeptin (3 μg/ml); pH 7.5]. After centrifugation at 15,000 rpm for 10 min at 4°C, the supernatant was collected and used for SDS–polyacrylamide gel electrophoresis (SDS-PAGE).

Institute of Cancer Research (ICR) mice were maintained at 25°C on a 14-hour light/10-hour dark cycle with free access to food and water. Mouse oocytes were isolated by puncturing ovaries with a needle in M2 medium [94.7 mM NaCl, 4.8 mM KCl, 1.7 mM $CaCl_2$, 1.2 mM KH_2PO_4, 1.2 mM $MgSO_4$, 4.2 mM $NaHCO_3$, 20.9 mM Hepes, 23.3 mM sodium lactate, 0.3 mM sodium pyruvate, 5.6 mM glucose, 0.1 mM gentamicin, phenol red (0.01 mg/ml), and bovine serum albumin (BSA) (4 mg/ml); pH 7.2 to 7.4] containing 10 μM milrinone as an inhibitor of the resumption of meiosis (M2+). Oocyte maturation was induced by incubating fully grown oocytes with M16 medium [94.7 mM NaCl, 4.8 mM KCl, 1.7 mM $CaCl_2$, 1.2 mM KH_2PO_4, 1.2 mM $MgSO_4$, 25.0 mM $NaHCO_3$, 20.9 mM Hepes, 23.3 mM sodium lactate, 0.3 mM sodium pyruvate, 5.6 mM glucose, 0.1 mM gentamicin, phenol red (0.01 mg/ml), and BSA (4 mg/ml); pH 7.2 to 7.4] under 5% CO_2 in air at 37°C. After incubation for 14 to 16 hours, oocytes extruding polar body were collected as mature oocytes. Embryos were collected after mating by flushing oviducts and/or uteri with phosphate-buffered saline (PBS; 137 mM NaCl, 2.70 mM KCl, 10.0 mM Na_2HPO_4, and 2.00 mM KH_2PO_4;pH 7.2). One-cell stage embryos were recovered from oviducts on day 1 of pregnancy, referred to as embryonic day (E) 0.5. Two-cell stage embryos were recovered from oviducts on day 2 of pregnancy (E1.5). For the PAT assay, oocytes and embryos were extracted with TRIzol reagent. For immunoblotting, 30 oocytes were washed with PBS and extracted with lithium dodecylsulfate sample buffer (Novex). For immunofluorescence, oocytes and embryos were fixed with 2% paraformaldehyde (PFA) in PBS for 20 min at room temperature.

PAT assay

RNA ligation–coupled RT-PCR was performed according to a previously reported procedure (*30*). Briefly, 2 μg of total RNA extracted from pools of 50 zebrafish oocytes or embryos was ligated to 0.4 μg of P1 anchor DNA primer (primer sequences are presented in table S3) in a 10-μl reaction mixture using T4 RNA ligase (New England Biolabs) for 30 min at 37°C. Similarly, 400 ng of total RNA extracted from pools of 200 to 300 mouse oocytes or embryos were ligated. The ligase was inactivated for 5 min at 92°C. Overall, 8 μl of the reaction mixture was used in a 10-μl reverse transcription reaction using SuperScript III First Strand Synthesis System (Invitrogen) with a P1′ primer. Then, 2 μl of the cDNA was used for the first round of PCR in a total volume of 25 μl with a P1′ primer and a primer specific for *pou5f3* (z*pou5f3*-PAT-f1), *wnt8a* (z*wnt8a*-PAT-f1), or *Pou5f1* (m*Pou5f1*-PAT-f1) for 17 to 20 cycles. Subsequently, 1 μl of the first-round PCR product was used for second-round PCR in a total volume of 25 μl with a P1′ primer and a primer specific for *pou5f3* (z*pou5f3*-PAT-f2), *wnt8a* (z*wnt8a*-PAT-f2), or *Pou5f1* (m*Pou5f1*-PAT-f2) for 30 to 35 cycles. To distinguish maternal and paternal mRNAs, we used z*pou5f3*-PAT-f3 and z*pou5f3*-PAT-f4 for the first and second rounds of PCR, respectively. To detect the 3′ ends of reporter mRNA, a primer specific for *GFP* gene (*GFP*-PAT-f1) was used instead of z*pou5f3*-PAT-f1 in the first-round PCR. The PCR products were then cloned into a pGEM-T vector (Promega), transformed into XL-1 cells, and sequenced. Last, >20 colonies were selected and sequenced for the quantitative assay.

Quantitative RT-PCR

pou5f3 mRNA was quantified in the early stages of embryos using a real-time PCR system with SYBR green PCR Master Mix (Applied Biosystems), according to the manufacturer′s instructions. Extracts from 50 embryos with EB containing recombinant ribonuclease (RNase) inhibitor (80 U/ml; Takara) were treated with proteinase K (10 μg/ml; Sigma-Aldrich) at 37°C for 2 hours. Total RNAs were extracted with TRIzol reagent and used for cDNA synthesis using SuperScript III First Strand Synthesis System. The *pou5f3* transcript was amplified with the cDNA and primer sets specific for *pou5f3* mRNA (table S3). The *foxa3*, *kazald2*, *cldne*, and β-*actin* transcripts were amplified using primer sets specific for distinct mRNAs (table S3). Similarly, the amounts of reporter and *eIf1*α mRNAs in transgenic fish were quantified using total RNAs extracted using the RNeasy Mini Kit (QIAGEN) and primer sets specific for *GFP* and *eIf1*α mRNAs (table S3). The level of reporter mRNAs was normalized to that of *eIf1*α mRNA.

Generation of transgenic zebrafish

Using pT2KXIGΔin (*78*), the GFP-*pou5f3* 3′UTR reporter genes were constructed by replacing the Ef1 promoter and SV40 3′UTR

with the heat shock promoter and *pou5f3* 3′UTRs, respectively. Transgenic zebrafish were generated using *Tol2* transposon-mediated germline transmission (*79*). Three lines carrying the same reporter gene were generated and analyzed. All lines carrying the same reporter gene gave equivalent results. Adult fish were heat-shocked via warming in a water bath at 38°C for 1 hour. For in situ hybridization analysis, embryos from distinct transgenic females were fixed at 2 hpf with 4% PFA in PBS overnight at 4°C. Whole-mount in situ hybridization of zebrafish embryos was performed according to a previously reported procedure (*30*).

Puromycylation followed by the proximity ligation assay

Puro-PLA was performed according to a previously reported procedure (*37*). To detect the Puro-PLA sites of the reporter mRNAs, anti-GFP rabbit antibody (Sigma-Aldrich, G1544) and anti-puromycin mouse antibody (Kerafast, 3RH11) were used. The samples were observed under an LSM 980 confocal microscope (Carl Zeiss). The number of Puro-PLA sites was quantified using the ImageJ software.

Luciferase assay

To construct luciferase-*Pou5f1* 3′UTR reporter mRNAs, the full-length (Long) and 9-nt-deleted (−9 nt) *Pou5f1* 3′UTRs were inserted downstream of the *firefly* luciferase gene in a pGL3-Basic vector (Promega). The sequences containing the *firefly* luciferase gene and *Pou5f1* 3′UTR were digested and ligated into the Xho I/Xba I sites of the pCS2 vector. Luciferase with 14-nt-deleted *Pou5f1* 3′UTR (-14nt) was generated using a KOD-Plus-Mutagenesis Kit (Toyobo) with luciferase-*Pou5f1* 3′UTR (Long) plasmid and the primer set m*Pou5f1*(-14nt)-f and m*Pou5f1*(mut)-r1 (table S3). Similarly, point mutations were generated at the 3′ end of *Pou5f1* using the forward primers m*Pou5f1*(2nt mut)-f, m*Pou5f1*(5nt mut)-f, and m*Pou5f1*(9nt mut)-f and the reverse primer m*Pou5f1*(mut)-r2. The 3′ end CACACAGUA sequence was mutated to CACAAAUUA (2-nt mutations), CACCACUGA (5-nt mutations), or ACACACUGC (9-nt mutations). The resulting plasmids were linearized with Xba I. The reporter mRNAs were synthesized using the mMESSAGE mMACHINE SP6 Transcription Kit (Ambion) and dissolved in nuclease-free distilled water. The mRNA of *Renilla* luciferase fused with the SV40 3′UTR was synthesized using mMESSAGE mMACHINE SP6 Transcription Kit, with pRL-CMV plasmid (Promega) linearized with Bam HI.

The solution containing mRNAs of *firefly* luciferase-*Pou5f1* 3′UTRs (50 ng/μl) and *Renilla* luciferase-SV40 poly(A) (25 ng/μl) were injected into immature mouse oocytes in M2+ medium using a microinjector (Dmi8; Leica). The oocytes were then incubated in M2+ medium for 2 hours. Overall, 50% of the mRNA-injected oocytes were incubated with M2 medium for 14 to 16 hours to allow for maturation. The remaining oocytes were maintained as immature oocytes in milrinone-containing M2 medium. After washing with PBS, 10 oocytes were collected and lysed in 10 μl of lysis buffer (Toyo Ink Inc.) for 15 min at room temperature. The Dual-Luciferase assay was conducted using the Pikka Gene Dual Assay Kit (Toyo Ink Inc.). In total, 10 μl of samples and 25 μl of luminescent reagent were used. Signal intensities were obtained using a TriStar LB 941 (Berthold Technologies). The intensity of firefly luciferase was normalized to that of *Renilla* luciferase.

Zebrafish genome editing

The guide RNA (gRNA) for modifying the *pou5f3* 3′ end was constructed using the GeneArt Precision gRNA Synthesis Kit (Invitrogen) with the primer set z*pou5f3*-gRNA-f and z*pou5f3*-gRNA-r (table S3). A mixture of gRNA (200 ng/μl) and TrueCut Cas9 Protein v2 (500 ng/μl; Invitrogen) was injected into the cytoplasm of fertilized zebrafish eggs. Mutations were analyzed using a previously described procedure (*80*). Briefly, injected embryos were extracted at 24 hpf and subjected to PCR with the primer set z*pou5f3*-genome-f and z*pou5f3*-genome-r (table S3). The amplification products were analyzed using the heteroduplex mobility assay (HMA) to confirm the presence of mutations at the 3′ end. Adult fish carrying mutations were analyzed by HMA after DNA extraction from fin clips. Fish heterozygous and homozygous for the mutations were isolated by HMA and sequencing of amplification products.

Immunoblotting

The crude extracts from wild-type and mutant zebrafish embryos were separated by SDS-PAGE, blotted onto an Immobilon membrane, and probed with anti-zebrafish Pou5f3 rabbit antibody (*37*) or anti-Rpl11 rabbit antibody (Abcam, ab79352). The crude extracts from mouse oocytes and embryos were separated by SDS-PAGE with Bolt 4 to 12% Bis-Tris Plus gels (Novex) and blotted onto the Immobilon membrane using a Bolt Mini Blot Module (Novex). The membranes were probed with anti–hnRNP D (this study), anti-Gemin5 (this study), or anti-Dhx9 mouse antibody (this study).

MO injection

The sequences of antisense MOs (Gene Tools, LLC) are presented in Fig. 5A. The 3′end-MO targets the terminal sequence of *pou5f3* mRNA 3′UTR, whereas the 5mm-MO (control) contains 5-nt mismatches. The *pou5f3*-ATG-MO specifically targets the translation initiation site of *pou5f3* mRNA's (*37*). Using Femtojet (Eppendorf), 1 nl of 3-ng/μl 3′end-MO or 5mm-MO was injected into fertilized eggs. Similarly, 1 nl of 1-ng/μl *pou5f3*-ATG-MO was injected into fertilized eggs. To quantify the long *pou5f3* mRNA, total RNAs were extracted from wild-type and 3′end-MO–injected embryos at 4 hpf and reverse-transcribed with a primer specific for long *pou5f3* 3′UTR (table S3).

RNA pull-down assay and mass spectrometry

The long and short types of zebrafish *pou5f3* 3′ ends were amplified by PCR using the forward primer z*pou5f3*-3′UTR-f and the reverse primer z*pou5f3*-3′UTR-r1 (for long 3′UTR) or z*pou5f3*-3′UTR-r2 (for short 3′UTR; table S3). The amplification products were cloned into the pGEM-T vector. The bromouridine (BrU)–labeled RNA probes consisting of *pou5f3* (long) or *pou5f3* (short) 3′UTR were synthesized using a Riboprobe in vitro Transcription Systems kit (Promega). The antisense RNA probe of *pou5f3* (long) was synthesized as a control. The RNA pull-down assay was performed using the RiboTrap Kit (MBL International) according to the manufacturer's instructions. Briefly, anti-BrdU antibody (MBL International) was conjugated with Protein A Sepharose beads (GE Healthcare) overnight at 4°C, followed by binding of the BrU-labeled RNA probes to the beads. After washing the beads, zebrafish oocyte extracts were treated with the RNA probes at 4°C for 2 hours. The samples were then washed with Wash Buffer

II (MBL International), eluted with elution buffer (MBL International), and subjected to SDS-PAGE. The gels were then subjected to silver staining using Silver Stain MS kit (Wako Pure Chemical Industries Ltd). The bands were excised from the gel and subjected to mass spectrometric analysis using Orbitrap Velos Pro (Thermo Fisher Scientific). For protein identification, MASCOT 2.5.1 was used for database search against NCBInr_*Danio rerio* (updated on 05 September 2017; 39,947 sequences). The results from each run were filtered with the peptide confidence value, and peptides exhibiting a false discovery rate of <1% were selected. In addition, proteins identical to the sequenced peptides with the rank1 values were selected. GO analysis was performed using DAVID Bioinformatics Resources 6.8.

Mouse long and short *Pou5f1* 3′ ends were amplified by PCR and cloned into the pGEM-T vector. The sense or antisense BrU-labeled RNA was synthesized as previously described. After conjugation of the RNA probes to Protein Sepharose beads, mouse ovary extracts were treated with the beads at 4°C for 2 hours. After washing, the retrieved proteins were detected by immunoblotting.

IP/RT-PCR

Mouse ovaries were homogenized with equal volumes of ice-cold EB containing 1% Tween 20 and RNase inhibitor (100 U/ml; Invitrogen). After centrifugation at 5000 rpm for 15 min at 4°C, the supernatant was collected and used for IP. Further, 40 μl of mouse ovary extracts was incubated with anti-HuR (Santa Cruz Biotechnology, sc-5261), anti-ELAVL2 (HuB; Proteintech, 14008-1-AP), or anti–hnRNP D (this study) mouse antibody and protein A or G Mag Sepharose (GE Healthcare) overnight at 4°C. The same volume of mouse IgG (Jackson ImmunoResearch) was used as a control. The samples were washed five times with EB containing 1% Tween 20. After extracting mRNAs from the beads using TRIzol reagent, RT-PCR was performed using primer sets specific for *Pou5f1* and α-*tubulin* (table S3). In total, 300 mouse embryos in the early two-cell stage were homogenized with 400 μl of ice-cold EB containing 1% Tween 20 and RNase inhibitor (100 U/ml). After being irradiated twice in a ultraviolet (UV) crosslinker (XL-1000, Funakoshi) under an energy setting of 86 mJ/cm^2, 200 μl of mouse embryo extracts was incubated with anti-Gemin5 or anti-Dhx9 mouse antibody and protein A Sepharose overnight at 4°C.

Reverse transcription PCR

Total RNAs from mouse ovaries and oocytes were extracted using TRIzol reagent. Reverse transcription was performed using FastGene Scriptase II (Nippon Genetics) and oligo(dT) primer. The *hnRNP D*, *Gemin5*, and *Dhx9* transcripts were amplified using the cDNA and specific primer sets (table S3).

Production of antibodies

DNA sequences encoding a part of mouse hnRNP D (amino acid residues 64 to 236), Gemin5 (amino acid residues 1250 to 1500), or Dhx9 (amino acid residues 100 to 200) were amplified by PCR and ligated into pGEX-KG vector at Eco RI/Sal I sites to produce glutathione *S*-transferase (GST)–tagged proteins. The recombinant proteins were expressed in *Escherichia coli* and purified by SDS-PAGE, followed by electroelution in Tris-glycine buffer without SDS. The purified proteins were dialyzed against 1 mM Hepes (pH 7.5), lyophilized, and then injected into two mice. The obtained antisera were affinity-purified with recombinant GST–hnRNP D, GST-Gemin5, or GST-Dhx9 protein electroblotted onto the Immobilon membrane.

Immunofluorescence

Immunofluorescence was performed according to a previously reported procedure (*36*). Oocytes and embryos were fixed with 2% PFA for 20 min followed by permeabilization in 0.25% Triton X-100 for 10 min at room temperature. The samples were then incubated with blocking/washing solution for 1 hour at room temperature and then incubated with anti-Pou5f1/Oct4 rabbit antibody (Abcam, ab181557), anti–hnRNP D mouse antibody, anti-Gemin5 mouse antibody, and anti-Dhx9 mouse antibody overnight at 4°C. The samples were washed with blocking/washing solution and then incubated for 1 hour at room temperature with Alexa Flour 488–conjugated anti-rabbit or mouse IgG secondary antibody (Molecular Probes). The samples were mounted with VECTASHIELD Mounting Medium with 4′,6-diamidino-2-phenylindole (DAPI) (Funakoshi) and observed under LSM 980 confocal microscope.

UV crosslinking assay

Mouse ovary extracts were incubated with anti-Gemin5 or anti-Dhx9 antibody and Protein A Sepharose beads overnight at 4°C. One microgram of BrU-labeled RNA was incubated with immunoprecipitated Gemin5 or Dhx9 protein for 15 min, and the reaction mixtures were irradiated twice in the UV crosslinker (XL-1000, Funakoshi) under an energy setting of 86 mJ/cm^2. After RNase treatment, samples were subjected to immunoblotting using anti-BrdU antibody.

Trim21-mediated protein degradation

pGEMHE-mCherry-mTrim21 (Addgene, #105522) was linearized with Asc I. *mCherry-Trim21* mRNA was synthesized using mMESSAGE mMACHINE T7 Transcription Kit (Ambion) and dissolved in nuclease-free distilled water. Overall, 8 pl of mRNA (200 ng/μl) was injected into immature mouse oocytes or one-cell stage embryos using IM-9B microinjector under the Dmi8 microscope. The samples were incubated in M2+ (oocytes) or M2− (zygotes) medium at 37°C for 3 hours to allow for mTrim21 protein expression. The solution containing anti–hnRNP D (200 ng/μl), anti-Gemin5 (100 ng/μl), or anti-Dhx9 antibody (500 ng/μl) was injected into mCherry-Trim21–expressing oocytes/zygotes. The oocytes were incubated in M2+ medium at 37°C for 16 hours and then analyzed by immunoblotting. The embryos were incubated in M16 medium containing 0.01 mM EDTA under 5% CO_2 at 37°C and were collected at an early period of the two-cell stage to analyze Pou5f1 expression by immunofluorescence. Whole-mount in situ hybridization of mouse embryos was performed in accordance with a previously reported procedure (*31*), with slight modifications. Early two-cell stage mouse embryos were fixed with 4% PFA for 30 min and then permeabilized with 2% Triton X-100 for 20 min at room temperature. The samples were hybridized with a solution containing a digoxigenin (DIG)-labeled RNA probe (1 ng/μl) and then treated with anti-DIG–horseradish peroxidase (HRP) antibody (Roche). Subsequently, the samples were treated with tyramide-fluorescein (Akoya Bio Inc.). The samples were washed before being mounted with VECTASHIELD Mounting Medium with DAPI (Funakoshi) and observed under the LSM 980 confocal microscope. The intensities of all signal in at least five

samples were measured using the ImageJ software and calculated as the total signal.

3′ end RNA sequencing

The 3′ end RNA sequencing was performed using the 3′ mRNA-Seq Library Prep Kit (Lexogen) according to the manufacturer's instructions. Briefly, 500 ng of total RNAs extracted from pools of 50 zebrafish embryos was used for cDNA synthesis with an oligo(dT) primer (from the kit). The second-strand DNA was synthesized using random primers (from the kit). The library was amplified to add the adaptor sequences for Illumina sequencing by PCR. Sequencing was performed by Macrogen Japan Co. using HiSeqX (Illumina). Reads were analyzed using the Bluebee genomics analysis platform and mapped onto the zebrafish genome (ensemble v11) using Integrative Genomics Viewer. To identify mRNAs harboring longer 3′ end sequences in fertilized eggs, which are shortened at 4 hpf, we counted individual reads mapped on each gene and calculated the percentages of reads for long and short 3′ ends in embryos at 0 and 4 hpf (table S2). In this assay, *P* values were calculated using Fisher's exact test (fig. S9 and table S2).

Statistical analysis

Statistical analyses were performed using R software (www.r-project.org). *P* values were calculated using Student's *t* test, Tukey's multiple comparison test, Dunnett's test, or Mann-Whitney's *U* test as indicated in respective figure legends. All data are presented as means ± SD of biological replicates or individual samples from two to five biological replicates. *P* values of <0.05 were considered to indicate statistical significance.

Supplementary Materials

This PDF file includes:
Figs. S1 to S10
Legends for tables S1 and S2
Table S3

Other Supplementary Material for this manuscript includes the following:
Tables S1 and S2

REFERENCES AND NOTES

1. S. Hocine, R. H. Singer, D. Grunwald, RNA processing and export. *Cold Spring Harb. Perspect. Biol.* **2**, a000752 (2010).
2. K. C. Martin, A. Ephrussi, mRNA localization: Gene expression in the spatial dimension. *Cell* **136**, 719–730 (2009).
3. N. Sonenberg, A. G. Hinnebusch, Regulation of translation initiation in eukaryotes: Mechanisms and biological targets. *Cell* **136**, 731–745 (2009).
4. A. R. Buxbaum, G. Haimovich, R. H. Singer, In the right place at the right time: Visualizing and understanding mRNA localization. *Nat. Rev. Mol. Cell Biol.* **16**, 95–109 (2015).
5. H. Aanes, C. L. Winata, C. H. Lin, J. P. Chen, K. G. Srinivasan, S. G. P. Lee, A. Y. M. Lim, H. S. Hajan, P. Collas, G. Bourque, Z. Gong, V. Korzh, P. Aleström, S. Mathavan, Zebrafish mRNA sequencing deciphers novelties in transcriptome dynamics during maternal to zygotic transition. *Genome Res.* **21**, 1328–1338 (2011).
6. J. Chen, C. Melton, N. Suh, J. S. Oh, K. Horner, F. Xie, C. Sette, R. Blelloch, M. Conti, Genome-wide analysis of translation reveals a critical role for deleted in azoospermia-like (*Dazl*) at the oocyte-to-zygote transition. *Genes Dev.* **25**, 755–766 (2011).
7. S. A. Harvey, I. Sealy, R. Kettleborough, F. Fenyes, R. White, D. Stemple, J. C. Smith, Identification of the zebrafish maternal and paternal transcriptomes. *Development* **140**, 2703–2710 (2013).
8. C. Zhang, M. Wang, Y. Li, Y. Zhang, Profiling and functional characterization of maternal mRNA translation during mouse maternal-to-zygotic transition. *Sci. Adv.* **8**, eabj3967 (2022).
9. T. Kotani, K. Maehata, N. Takei, Regulation of translationally repressed mRNAs in zebrafish and mouse oocytes. *Results Probl. Cell Differ.* **63**, 297–324 (2017).
10. C. L. Winata, V. Korzh, The translational regulation of maternal mRNAs in time and space. *FEBS Lett.* **592**, 3007–3023 (2018).
11. T. Hamatani, M. G. Carter, A. A. Sharov, M. S. H. Ko, Dynamics of global gene expression changes during mouse preimplantation development. *Dev. Cell* **6**, 117–131 (2004).
12. D. A. Kane, C. B. Kimmel, The zebrafish midblastula transition. *Development* **119**, 447–456 (1993).
13. F. Aoki, K. T. Hara, R. M. Schultz, Acquisition of transcriptional competence in the 1-cell mouse embryo: Requirement for recruitment of maternal mRNAs. *Mol. Reprod. Dev.* **64**, 270–274 (2003).
14. P. Kumari, P. C. Gilligan, S. Lim, L. D. Tran, S. Winkler, R. Philp, K. Sampath, An essential role for maternal control of Nodal signaling. *eLife* **2**, e00683 (2013).
15. J. Sun, L. Yan, W. Shen, A. Meng, Maternal *ybx1* safeguards zebrafish oocyte maturation and maternal-to-zygotic transition by repressing global translation. *Development* **145**, dev166587 (2018).
16. Q. Wang, K. E. Latham, Requirement for protein synthesis during embryonic genome activation in mice. *Mol. Reprod. Dev.* **47**, 265–270 (1997).
17. C. L. Winata, M. Łapinski, L. Pryszcz, C. Vaz, M. H. Bin Ismail, S. Nama, H. S. Hajan, S. G. P. Lee, V. Korzh, P. Sampath, V. Tanavde, S. Mathavan, Cytoplasmic polyadenylation-mediated translational control of maternal mRNAs directs maternal-to-zygotic transition. *Development* **145**, dev159566 (2018).
18. T. Hultin, The effect of puromycin on protein metabolism and cell division in fertilized sea urchin eggs. *Experientia* **17**, 410–411 (1961).
19. M. Nemer, Interrelation of messenger polyribonucleotides and ribosomes in the sea urchin egg during embryonic development. *Biochem. Biophys. Res. Commun.* **8**, 511–515 (1962).
20. P. R. Gross, L. I. Malkin, W. A. Moyer, Templates for the first proteins of embryonic development. *Proc. Natl. Acad. Sci. U.S.A.* **51**, 407–414 (1964).
21. M. B. Dworkin, E. Dworkin-Rastl, Changes in RNA titers and polyadenylation during oogenesis and oocyte maturation in Xenopus laevis. *Dev. Biol.* **112**, 451–457 (1985).
22. C. A. Fox, M. D. Sheets, M. P. Wickens, Poly(A) addition during maturation of frog oocytes: Distinct nuclear and cytoplasmic activities and regulation by the sequence UUUUUAU. *Genes Dev.* **3**, 2151–2162 (1989).
23. L. L. McGrew, E. Dworkin-Rastl, M. B. Dworkin, J. D. Richter, Poly(A) elongation during Xenopus oocyte maturation is required for translational recruitment and is mediated by a short sequence element. *Genes Dev.* **3**, 803–815 (1989).
24. M. D. Sheets, C. A. Fox, T. Hunt, G. Vande Woude, M. Wickens, The 3′-untranslated regions of c-*mos* and cyclin mRNAs stimulate translation by regulating cytoplasmic polyadenylation. *Genes Dev.* **8**, 926–938 (1994).
25. M. Wickens, In the beginning is the end: Regulation of poly(A) addition and removal during early development. *Trends Biochem. Sci.* **15**, 320–324 (1990).
26. R. Mendez, J. D. Richter, Translational control by CPEB: A means to the end. *Nat. Rev. Mol. Cell Biol.* **2**, 521–529 (2001).
27. A. Charlesworth, A. Wilczynska, P. Thampi, L. L. Cox, A. M. MacNicol, Musashi regulates the temporal order of mRNA translation during Xenopus oocyte maturation. *EMBO J.* **25**, 2792–2801 (2006).
28. M. Pique, J. M. Lopez, S. Foissac, R. Guigo, R. Mendez, A combinatorial code for CPE-mediated translational control. *Cell* **132**, 434–448 (2008).
29. K. Arumugam, Y. Wang, L. L. Hardy, M. C. MacNicol, A. M. MacNicol, Enforcing temporal control of maternal mRNA translation during oocyte cell-cycle progression. *EMBO J.* **29**, 387–397 (2010).
30. T. Kotani, K. Yasuda, R. Ota, M. Yamashita, *Cyclin B1* mRNA translation is temporally controlled through formation and disassembly of RNA granules. *J. Cell Biol.* **202**, 1041–1055 (2013).
31. N. Takei, Y. Takada, S. Kawamura, K. Sato, A. Saitoh, J. Bormann, W. S. Yuen, J. Carroll, T. Kotani, Changes in subcellular structures and states of pumilio 1 regulate the translation of target *Mad2* and cyclin B1 mRNAs. *J. Cell Sci.* **133**, jcs249128 (2020).
32. N. Takei, K. Sato, Y. Takada, R. Iyyappan, A. Susor, T. Yamamoto, T. Kotani, Tdrd3 regulates the progression of meiosis II through translational control of *Emi2* mRNA in mouse oocytes. *Curr. Res. Cell Biol.* **2**, 100009 (2021).
33. H. Takeda, T. Matsuzaki, T. Oki, T. Miyagawa, H. Amanuma, A novel POU domain gene, zebrafish *pou2*: Expression and roles of two alternatively spliced twin products in early development. *Genes Dev.* **8**, 45–59 (1994).
34. H. R. Scholer, S. Ruppert, N. Suzuki, K. Chowdhury, P. Gruss, New type of POU domain in germ line-specific protein Oct-4. *Nature* **344**, 435–439 (1990).

35. K. Okamoto, H. Okazawa, A. Okuda, M. Sakai, M. Muramatsu, H. Hamada, A novel octamer binding transcription factor is differentially expressed in mouse embryonic cells. *Cell* **60**, 461–472 (1990).
36. Y. Takada, R. Iyyappan, A. Susor, T. Kotani, Posttranscriptional regulation of maternal *Pou5f1/Oct4* during mouse oogenesis and early embryogenesis. *Histochem. Cell Biol.* **154**, 609–620 (2020).
37. K. Sato, M. Sakai, A. Ishii, K. Maehata, Y. Takada, K. Yasuda, T. Kotani, Identification of embryonic RNA granules that act as sites of mRNA translation after changing their physical properties. *iScience* **25**, 104344 (2022).
38. K. Lunde, H. G. Belting, W. Driever, Zebrafish *pou5f1/pou2*, homolog of mammalian *Oct4*, functions in the endoderm specification cascade. *Curr. Biol.* **14**, 48–55 (2004).
39. G. Reim, M. Brand, Maternal control of vertebrate dorsoventral axis formation and epiboly by the POU domain protein *Spg*/*Pou2*/Oct4. *Development* **133**, 2757–2770 (2006).
40. G. Reim, T. Mizoguchi, D. Y. Stainier, Y. Kikuchi, M. Brand, The POU domain protein *spg* (*pou2*/*Oct4*) is essential for endoderm formation in cooperation with the HMG domain protein casanova. *Dev. Cell* **6**, 91–101 (2004).
41. M. T. Lee, A. R. Bonneau, C. M. Takacs, A. A. Bazzini, K. R. DiVito, E. S. Fleming, A. J. Giraldez, Nanog, Pou5f1 and SoxB1 activate zygotic gene expression during the maternal-to-zygotic transition. *Nature* **503**, 360–364 (2013).
42. M. Leichsenring, J. Maes, R. Mossner, W. Driever, D. Onichtchouk, Pou5f1 transcription factor controls zygotic gene activation in vertebrates. *Science* **341**, 1005–1009 (2013).
43. B. Lippok, S. Song, W. Driever, Pou5f1 protein expression and posttranslational modification during early zebrafish development. *Dev. Dyn.* **243**, 468–477 (2014).
44. R. J. White, J. E. Collins, I. M. Sealy, N. Wali, C. M. Dooley, Z. Digby, D. L. Stemple, D. N. Murphy, K. Billis, T. Hourlier, A. Füllgrabe, M. P. Davis, A. J. Enright, E. M. Busch-Nentwich, A high-resolution mRNA expression time course of embryonic development in zebrafish. *eLife* **6**, e30860 (2017).
45. F. I. Lu, C. Thisse, B. Thisse, Identification and mechanism of regulation of the zebrafish dorsal determinant. *Proc. Natl. Acad. Sci. U.S.A.* **108**, 15876–15880 (2011).
46. S. tom Dieck, L. Kochen, C. Hanus, M. Heumüller, I. Bartnik, B. Nassim-Assir, K. Merk, T. Mosler, S. Garg, S. Bunse, D. A. Tirrell, E. M. Schuman, Direct visualization of newly synthesized target proteins in situ. *Nat. Methods* **12**, 411–414 (2015).
47. A. B. Cubitt, R. Heim, S. R. Adams, A. E. Boyd, L. A. Gross, R. Y. Tsien, Understanding, improving and using green fluorescent proteins. *Trends Biochem. Sci.* **20**, 448–455 (1995).
48. C. Colombrita, V. Silani, A. Ratti, ELAV proteins along evolution: Back to the nucleus? *Mol. Cell. Neurosci.* **56**, 447–455 (2013).
49. D. Clift, W. A. McEwan, L. I. Labzin, V. Konieczny, B. Mogessie, L. C. James, M. Schuh, A method for the acute and rapid degradation of endogenous proteins. *Cell* **172**, 1692–1706 e1618 (2017).
50. G. Dreyfuss, V. N. Kim, N. Kataoka, Messenger-RNA-binding proteins and the messages they carry. *Nat. Rev. Mol. Cell Biol.* **3**, 195–205 (2002).
51. D. J. Battle, C. K. Lau, L. Wan, H. Deng, F. Lotti, G. Dreyfuss, The Gemin5 protein of the SMN complex identifies snRNAs. *Mol. Cell* **23**, 273–279 (2006).
52. A. Pacheco, S. López de Quinto, J. Ramajo, N. Fernández, E. Martínez-Salas, A novel role for Gemin5 in mRNA translation. *Nucleic Acids Res.* **37**, 582–590 (2009).
53. T. Lee, J. Pelletier, The biology of DHX9 and its potential as a therapeutic target. *Oncotarget* **7**, 42716–42739 (2016).
54. L. A. Passmore, J. Coller, Roles of mRNA poly(A) tails in regulation of eukaryotic gene expression. *Nat. Rev. Mol. Cell Biol.* **23**, 93–106 (2022).
55. C. J. Decker, R. Parker, A turnover pathway for both stable and unstable mRNAs in yeast: Evidence for a requirement for deadenylation. *Genes Dev.* **7**, 1632–1643 (1993).
56. A. Yamashita, T.-C. Chang, Y. Yamashita, W. Zhu, Z. Zhong, C.-Y. A. Chen, A.-B. Shyu, Concerted action of poly(A) nucleases and decapping enzyme in mammalian mRNA turnover. *Nat. Struct. Mol. Biol.* **12**, 1054–1063 (2005).
57. A. C. Goldstrohm, M. Wickens, Multifunctional deadenylase complexes diversify mRNA control. *Nat. Rev. Mol. Cell Biol.* **9**, 337–344 (2008).
58. Y. Mishima, Y. Tomari, Codon usage and 3′ UTR length determine maternal mRNA stability in zebrafish. *Mol. Cell* **61**, 874–885 (2016).
59. C. Yu, S. Y. Ji, Q. Q. Sha, Y. Dang, J. J. Zhou, Y. L. Zhang, Y. Liu, Z. W. Wang, B. Hu, Q. Y. Sun, S. C. Sun, F. Tang, H. Y. Fan, BTG4 is a meiotic cell cycle-coupled maternal-zygotic-transition licensing factor in oocytes. *Nat. Struct. Mol. Biol.* **23**, 387–394 (2016).
60. S. Thore, F. Mauxion, B. Séraphin, D. Suck, X-ray structure and activity of the yeast Pop2 protein: A nuclease subunit of the mRNA deadenylase complex. *EMBO Rep.* **4**, 1150–1155 (2003).
61. C. Bianchin, F. Mauxion, S. Sentis, B. Séraphin, L. Corbo, Conservation of the deadenylase activity of proteins of the Caf1 family in human. *RNA* **11**, 487–494 (2005).
62. Y. Q. Su, K. Sugiura, Y. Woo, K. Wigglesworth, S. Kamdar, J. Affourtit, J. J. Eppig, Selective degradation of transcripts during meiotic maturation of mouse oocytes. *Dev. Biol.* **302**, 104–117 (2007).
63. Z. Ji, J. Y. Lee, Z. Pan, B. Jiang, B. Tian, Progressive lengthening of 3′ untranslated regions of mRNAs by alternative polyadenylation during mouse embryonic development. *Proc. Natl. Acad. Sci. U.S.A.* **106**, 7028–7033 (2009).
64. I. Ulitsky, A. Shkumatava, C. H. Jan, A. O. Subtelny, D. Koppstein, G. W. Bell, H. Sive, D. P. Bartel, Extensive alternative polyadenylation during zebrafish development. *Genome Res.* **22**, 2054–2066 (2012).
65. K. Foygel, B. Choi, S. Jun, D. E. Leong, A. Lee, C. C. Wong, E. Zuo, M. Eckart, R. A. R. Pera, W. H. Wong, M. W. M. Yao, A novel and critical role for Oct4 as a regulator of the maternal-embryonic transition. *PLOS ONE* **3**, e4109 (2008).
66. A. Fukuda, A. Mitani, T. Miyashita, H. Kobayashi, A. Umezawa, H. Akutsu, Spatiotemporal dynamics of OCT4 protein localization during preimplantation development in mice. *Reproduction* **152**, 417–430 (2016).
67. G. Marsboom, G. F. Zhang, N. Pohl-Avila, Y. Zhang, Y. Yuan, H. Kang, B. Hao, H. Brunengraber, A. B. Malik, J. Rehman, Glutamine metabolism regulates the pluripotency transcription factor OCT4. *Cell Rep.* **16**, 323–332 (2016).
68. J. H. Kim, J. D. Richter, Opposing polymerase-deadenylase activities regulate cytoplasmic polyadenylation. *Mol. Cell* **24**, 173–183 (2006).
69. R. Mendez, D. Barnard, J. D. Richter, Differential mRNA translation and meiotic progression require Cdc2-mediated CPEB destruction. *EMBO J.* **21**, 1833–1844 (2002).
70. Q. Cao, J. D. Richter, Dissolution of the maskin-eIF4E complex by cytoplasmic polyadenylation and poly(A)-binding protein controls cyclin B1 mRNA translation and oocyte maturation. *EMBO J.* **21**, 3852–3862 (2002).
71. W. Zhang, B. J. Wagner, K. Ehrenman, A. W. Schaefer, C. T. DeMaria, D. Crater, K. DeHaven, L. Long, G. Brewer, Purification, characterization, and cDNA cloning of an AU-rich element RNA-binding protein, AUF1. *Mol. Cell. Biol.* **13**, 7652–7665 (1993).
72. X. Cui, C. Hao, L. Gong, N. Kajitani, S. Schwartz, HnRNP D activates production of HPV16 E1 and E6 mRNAs by promoting intron retention. *Nucleic Acids Res.* **50**, 2782–2806 (2022).
73. E. Workman, C. Kalda, A. Patel, D. J. Battle, Gemin5 binds to the survival motor neuron mRNA to regulate SMN expression. *J. Biol. Chem.* **290**, 15662–15669 (2015).
74. T. R. Hartman, S. Qian, C. Bolinger, S. Fernandez, D. R. Schoenberg, K. Boris-Lawrie, RNA helicase A is necessary for translation of selected messenger RNAs. *Nat. Struct. Mol. Biol.* **13**, 509–516 (2006).
75. J. Jin, W. Jing, X.-X. Lei, C. Feng, S. Peng, K. Boris-Lawrie, Y. Huang, Evidence that Lin28 stimulates translation by recruiting RNA helicase A to polysomes. *Nucleic Acids Res.* **39**, 3724–3734 (2011).
76. R. Francisco-Velilla, J. Fernandez-Chamorro, J. Ramajo, E. Martinez-Salas, The RNA-binding protein Gemin5 binds directly to the ribosome and regulates global translation. *Nucleic Acids Res.* **44**, 8335–8351 (2016).
77. K. Fujimura, J. Katahira, F. Kano, Y. Yoneda, M. Murata, Microscopic dissection of the process of stress granule assembly. *Biochim. Biophys. Acta* **1793**, 1728–1737 (2009).
78. K. Kawakami, H. Takeda, N. Kawakami, M. Kobayashi, N. Matsuda, M. Mishina, A transposon-mediated gene trap approach identifies developmentally regulated genes in zebrafish. *Dev. Cell* **7**, 133–144 (2004).
79. T. Kotani, S. Nagayoshi, A. Urasaki, K. Kawakami, Transposon-mediated gene trapping in zebrafish. *Methods* **39**, 199–206 (2006).
80. E. L. Sorlien, M. A. Witucki, J. Ogas, Efficient production and identification of CRISPR/Cas9-generated gene knockouts in the model system *Danio rerio*. *J. Vis. Exp.* **138**, e56969 (2018).

Acknowledgments: We thank Y. Mishima at Kyoto Sangyo University for valuable discussion on deadenylases, K. Maehata for an initial experiment of the PAT assay, and Zebrafish International Resource Center for providing Tübingen wild-type zebrafish. **Funding:** This work was supported by Grant-in-Aid for Scientific Research KAKENHI grant numbers 16K07242 and 21H02398 (to T.K.) from Japan Society for the Promotion of Science (JSPS) and was in part supported by grant from Mochida Memorial Foundation for Medical and Pharmaceutical Research. This work was partially performed in the Cooperative Research Project Program of the Medical Institute of Bioregulation, Kyushu University. **Author contributions:** Conceptualization: Y.T. and T.K. Investigation: Y.T., L.F., K.S., T.S., and A.I. Resources: T.Y. Supervision and funding acquisition: T.K. Writing: Y.T. and T.K. **Competing interests:** The authors declare that they have no competing interests. **Data and materials availability:** All data needed to evaluate the conclusions in the paper are present in the paper and/or the Supplementary Materials.

Submitted 13 January 2023
Accepted 25 October 2023
Published 24 November 2023
10.1126/sciadv.adg6532